QuadMath: An Analytical Review of 4D and Quadray Coordinates

Daniel Ari Friedman
ORCID: 0000-0001-6232-9096
Email: daniel@activeinference.institute

August 15, 2025

Contents

1 QuadMath: An Analytical Review of 4D and Quadray Coordinates

1.1 Abstract

We review a unified analytical framework for four dimensional (4D) modeling and Quadray coordinates, synthesizing geometric foundations, optimization on tetrahedral lattices, and information geometry. Building on R. Buckminster Fuller's Synergetics and the Quadray coordinate system, with extensive reference to Kirby Urner's computational implementations across multiple programming languages (see the comprehensive 4dsolutions ecosystem including Python, Rust, Clojure, and POV-Ray implementations), we review how integer lattice constraints yield integer volume quantization of tetrahedral simplexes, creating discrete "energy levels" that regularize optimization and enable integer-based optimization. We adapt standard methods (e.g., Nelder–Mead method) to the quadray lattice, define Fisher information in Quadray parameter space, and analyze optimization as geodesic motion on an information manifold via the natural gradient. We review three distinct 4D namespaces — Coxeter.4D (Euclidean E^4), Einstein.4D (Minkowski spacetime), and Fuller.4D (synergetics/Quadrays) — develop analytical tools and equations, and survey extensions and applications across AI, active inference, cognitive security, and complex systems. The result is a cohesive, interpretable approach for robust, geometry-grounded computation in 4D. All source code for the manuscript is available at QuadMath. The future is open source and 4D!

Keywords: Quadray coordinates, 4D geometry, tetrahedral lattice, integer volume quantization, information geometry, optimization, synergetics, active inference.

1.2 Manuscript structure

- Introduction: motivates Quadrays, clarifies 4D namespaces (Coxeter.4D, Einstein.4D, Fuller.4D), and summarizes contributions.
- Methods: details coordinate conventions, exact tetravolumes, conversions, and lattice-aware optimization methods (Nelder–Mead and discrete IVM descent).
- Results: empirical comparisons and demonstrations are shown inline and saved under `quadmath/output/` (PNG/CSV/NPZ/MP4) for reproducibility.
- Discussion: interprets results, limitations, and implications; outlines future work.
- Appendices: equations, free-energy background, and a consolidated symbols/glossary with an auto-generated API index.

1.3 Reproducibility and data availability

- The manuscript Markdown and code to generate the PDF are available on the project repository (`QuadMath` on GitHub, @docxology username). See the repository home page for source, figures, and scripts: QuadMath repository.
- The manuscript is licensed under the Apache License 2.0. See the LICENSE file for details.
- The manuscript is accompanied by a fully-tested Python codebase under `src/` with unit tests under `tests/`, complemented by extensive cross-validation against Kirby Urner's reference implementations in the 4dsolutions ecosystem. See the Resources section for comprehensive details on computational implementations and validation.
- All figures referenced in the manuscript are generated by scripts under `quadmath/scripts/` and saved to `quadmath/output/` with lightweight CSV/NPZ alongside images.
- Tests accompany all methods under `src/` and enforce 100% coverage for `src/`.
- Symbols and notation are standardized across sections; see Appendix: Symbols and Glossary for a consolidated table of variables and constants used throughout. Equation labels (e.g., Eq. (14) and Eq. (17)) and figure labels are automatically numbered by LaTeX for consistent cross-referencing.

2 Introduction

Quadray coordinates provide a tetrahedral basis for modeling space and computation, standing in contrast to Cartesian cubic frameworks. Originating in Buckminster Fuller's Synergetics, quadray coordinates enable the replacement of right-angle orthonormal assumptions, with 60-degree coordination and a unit tetrahedron of volume 1. This reframing yields striking integer relationships among common polyhedra and provides a natural account of space via close-packed spheres and the isotropic vector matrix (IVM).

In this synthetic review, we distinguish three internal meanings of “4D,” following a dot-notation that avoids cross-domain confusion:

- **Coxeter.4D** — four-dimensional Euclidean space (E^4), as in classical polytope theory. Coxeter emphasizes that Euclidean 4D is not spacetime; see the Dover edition of Regular Polytopes (p. 119) for a clear statement to this effect; background on lattice packings in four dimensions aligns with the treatment in Conway & Sloane’s Sphere Packings, Lattices and Groups.
- **Einstein.4D** — Minkowski spacetime (3D + time) with an indefinite metric; appropriate for relativistic physics but distinct from Euclidean E^4.
- **Fuller.4D** — synergetics’ tetrahedral accounting of space using Quadrays (four non-negative coordinates with at least one zero after normalization) and the Isotropic Vector Matrix (IVM) = Cubic Close Packing (CCP) = Face-Centered Cubic (FCC) correspondence. This treats the regular tetrahedron as a natural unit container and emphasizes angle/shape relations independent of time/energy.

This paper unifies three threads:

- **Foundations**: Quadray coordinates and their relation to 4D modeling more generally, with explicit namespace usage (Coxeter.4D, Einstein.4D, Fuller.4D) to maintain clarity.
- **Optimization framework**: leverages integer volume quantization on tetrahedral lattices to achieve robust, discrete convergence.
- **Information geometry**: tools (e.g., Fisher Information, free-energy minimization) for interpreting optimization as geodesic motion on statistical manifolds.

Contributions:

- **Namespaces mapping**: Coxeter.4D (Euclidean E^4), Einstein.4D (Minkowski spacetime), and Fuller.4D (Quadrays/IVM) → analytical tools and examples.
- **Quadray-adapted Nelder–Mead**: integer-lattice normalization and volume-level tracking.
- **Equations and methods**: comprehensive supplement with guidance for high-precision computation using `libquadmath`.
- **Discrete optimizer**: integer-valued variational descent over the IVM (`discrete_ivm_descent`) with animation tooling, connecting lattice geometry to information-theoretic objectives.

2.1 Companion code and tests

The manuscript is accompanied by a fully-tested Python codebase under `src/` with unit tests under `tests/`. Key artifacts used throughout the paper:

- **Quadray APIs**: `src/quadray.py` (`Quadray`, `integer_tetra_volume`, `ace_tetravolume_5x5`).
- **Determinant utilities**: `src/linalg_utils.py` (`bareiss_determinant_int`).
- **Length-based volume**: `src/cayley_menger.py` (`tetra_volume_cayley_menger`, `ivm_tetra_volume_cayley_menger`).
- **XYZ conversion**: `src/conversions.py` (`urner_embedding`, `quadray_to_xyz`).
- **Examples**: `src/examples.py` (`example_ivm_neighbors`, `example_volume`, `example_optimize`).

For comprehensive background resources, computational implementations, and related work, see the Resources section.

Graphical abstract: Panel A shows Quadray axes (A,B,C,D) under a symmetric embedding with wireframe context. Panel B shows close-packed spheres at the tetrahedron vertices (IVM/CCP/FCC, “twelve around one”).

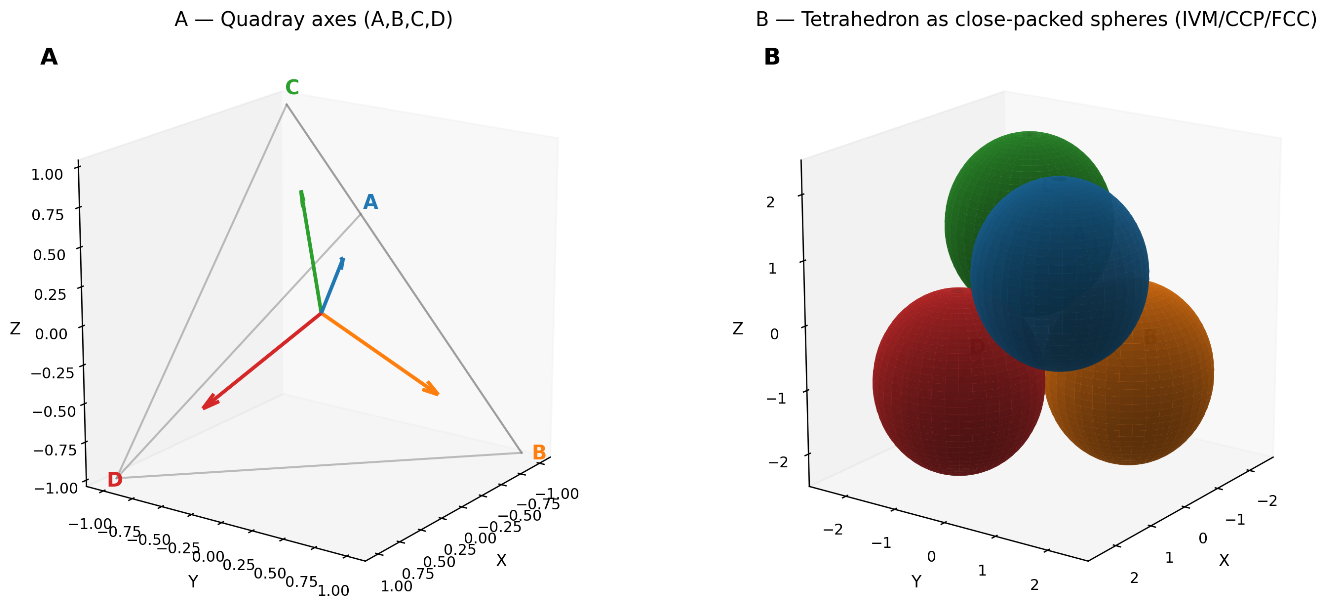
A — Quadray axes (A,B,C,D)
A
C
A
B
D
Z
Y
X
B — Tetrahedron as close-packed spheres (IVM/CCP/FCC)
B
Z
Y
X

3 4D Namespaces: Coxeter.4D, Einstein.4D, Fuller.4D

In this section, we clarify the three internal meanings of “4D,” following a dot-notation that avoids cross-domain confusion. Each namespace represents a distinct mathematical framework with specific applications in our quadray-based computational system.

3.1 Coxeter.4D (Euclidean E^4)

- **Definition**: Standard E^4 with orthogonal axes and Euclidean metric; the proper setting for classical regular polytopes. As Coxeter notes (Regular Polytopes, Dover ed., p. 119), this Euclidean 4D is not spacetime. Lattice/packing discussions connect to Conway & Sloane’s systematic treatment of higher-dimensional sphere packings and lattices (Sphere Packings, Lattices and Groups (Springer)).
- **Usage**: Embed Quadray configurations or compare alternative parameterizations when a strictly Euclidean 4D setting is desired.
- **Simplexes**: Simplex structures extend naturally to 4D and beyond (e.g., pentachora).
- **Mathematical context**: This framework is appropriate for standard Euclidean geometry, including the Cayley-Menger determinant for computing volumes from edge lengths.

3.2 Einstein.4D (Relativistic spacetime)

- **Spacetime**: Minkowski metric signature.
- **Line element** (mostly-plus convention; see Minkowski space):

$$ds^2 = -c^2\,dt^2 + dx^2 + dy^2 + dz^2 \tag{1}$$

- **Optimization analogy**: Metric-aware geodesics generalize to information geometry where the Fisher metric replaces the physical metric. See Fisher information and natural gradient.
- **Important note**: This namespace is used ONLY as a metric/geodesic analogy when discussing information geometry. Physical constants G, c, Λ do not appear in Quadray lattice methods and should not be mixed with IVM unit conventions.

3.3 Fuller.4D (Synergetics / Quadrays)

- **Basis**: Four non-negative components A,B,C,D with at least one zero post-normalization, treated as a vector (direction and magnitude), not merely a point. Overview: Quadray coordinates.
- **Geometry**: Tetrahedral; unit tetrahedron volume = 1; integer lattice aligns with close-packed spheres (IVM). Background: Synergetics.
- **Distances**: Computed via appropriate projective normalization; edges align with tetrahedral axes. The IVM = CCP = FCC shortcut allows working in 3D embeddings for visualization while preserving the underlying Fuller.4D tetrahedral accounting.
- **Implementation heritage**: Extensive computational validation through Kirby Urner's 4dsolutions ecosystem. See the Resources section for comprehensive details on computational implementations and educational materials.

3.3.1 Directions, not dimensions (language and models)

- **Vector-first framing**: Treat Quadrays as four canonical directions ("spokes" to the vertices of a regular tetrahedron from its center), not as four orthogonal dimensions. The methane molecule (CH_4) and caltrop shape are helpful mental models.
- **Origins outside Synergetics**: Quadrays did not originate with Fuller; we adopt the coordinate system within the IVM context. See Quadray coordinates.
- **Language games**: Quadrays and Cartesian are parallel vector languages on the same Euclidean container; teaching them together avoids oscillating between "points now, vectors later."

3.3.2 Figures

In the previous figure, we show the twelve nearest IVM neighbors with coordination patterns and vector equilibrium geometry; the current figure illustrates random Quadray clouds under several embeddings.

Vector equilibrium (cuboctahedron). The shell formed by the 12 nearest IVM neighbors is the cuboctahedron, also called the vector equilibrium in synergetics. All 12 vertices are equidistant from the origin with equal edge lengths, modeling a balanced local packing. This geometry underlies the "twelve around one" close-packing motif and appears in tensegrity discussions as a canonical balanced structure. See background: Cuboctahedron (vector equilibrium) and synergetics references. Computational demonstrations include related visualizations in the 4dsolutions ecosystem. See the Resources section for comprehensive details.

3.3.3 Clarifying remarks

- "A time machine is not a tesseract." KU on synergeo The tesseract is a Euclidean 4D object (Coxeter.4D), while Minkowski spacetime (Einstein.4D) is indefinite and not Euclidean; conflating the two leads to category errors. Fuller.4D, in turn, is a tetrahedral, mereological framing of ordinary space emphasizing shape/angle relations and IVM quantization. Each namespace carries distinct assumptions and should be used accordingly in analysis.

3.4 Practical usage guide

- Use **Fuller.4D** when working with Quadrays, integer tetravolumes, and IVM neighbors (native lattice calculations).
- Use **Coxeter.4D** for Euclidean length-based formulas, higher-dimensional polytopes, or comparisons in E^4 (including Cayley–Menger).
- Use **Einstein.4D** as a metric analogy when discussing geodesics or time-evolution; do not mix with synergetic unit conventions.

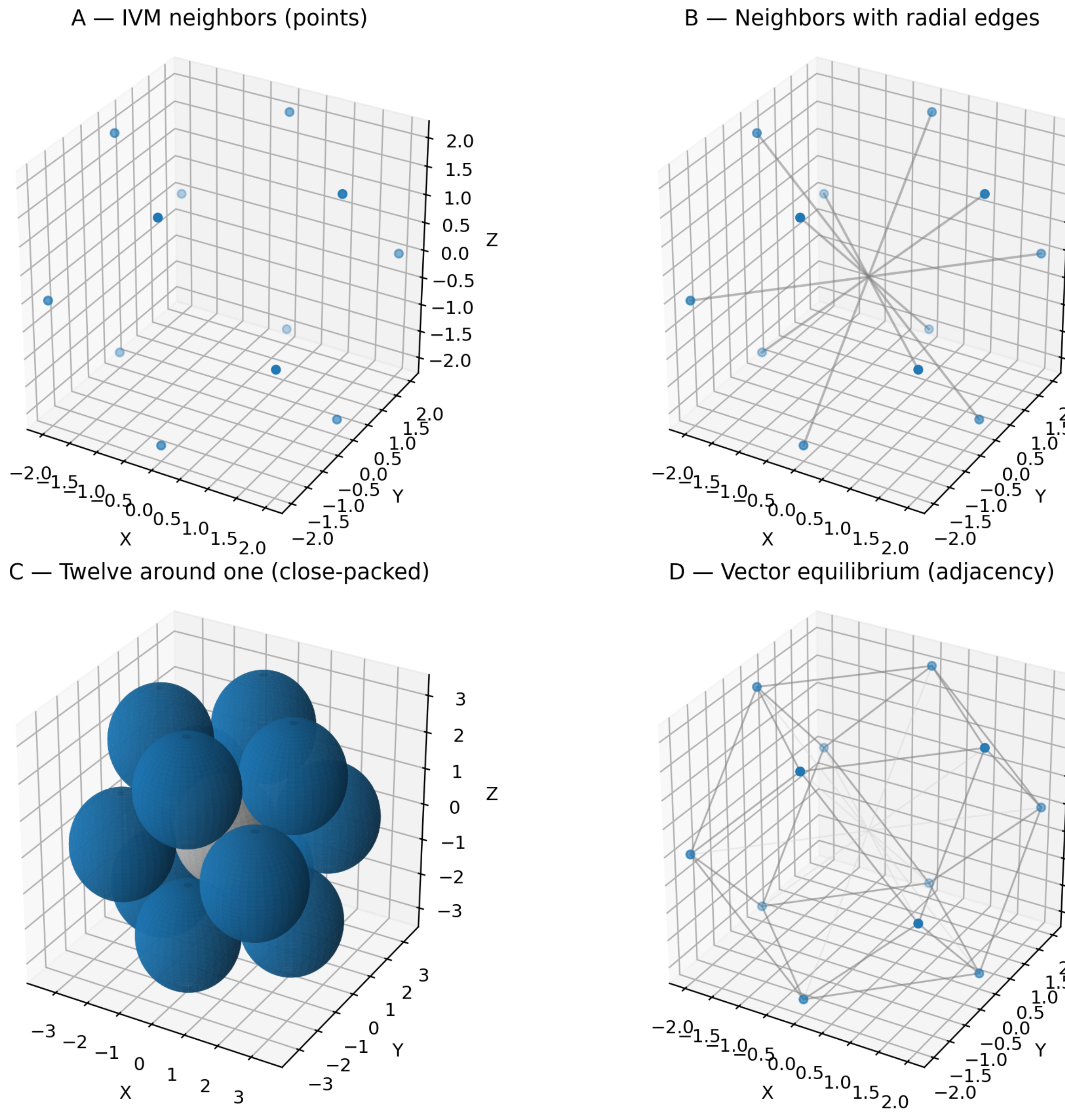

Figure 1: **IVM neighbors and coordination patterns (2×2 panel layout)**. **Panel A**: The twelve nearest IVM neighbors plotted as blue points in 3D space under the default embedding, showing the positions corresponding to permutations of the Quadray integer coordinates {2,1,1,0}. These points form the vertices of a cuboctahedron (vector equilibrium) centered at the origin with uniform radial distances. **Panel B**: The same neighbor points with radial edges (light lines) connecting each neighbor to the central origin, emphasizing the spoke-like radial symmetry and equal distances from center to shell. **Panel C**: Twelve-around-one close-packed spheres configuration where each neighbor position hosts a sphere with radius chosen so neighboring spheres kiss along cuboctahedron edges, illustrating the fundamental CCP/FCC/IVM correspondence. The central gray sphere represents the "one" in Fuller's "twelve around one" motif. **Panel D**: Adjacency graph showing strut connections (solid lines) between touching neighbor spheres, revealing the cuboctahedron's edge structure, plus light radial cables to the origin representing a stylized tensegrity interpretation of the vector equilibrium geometry.

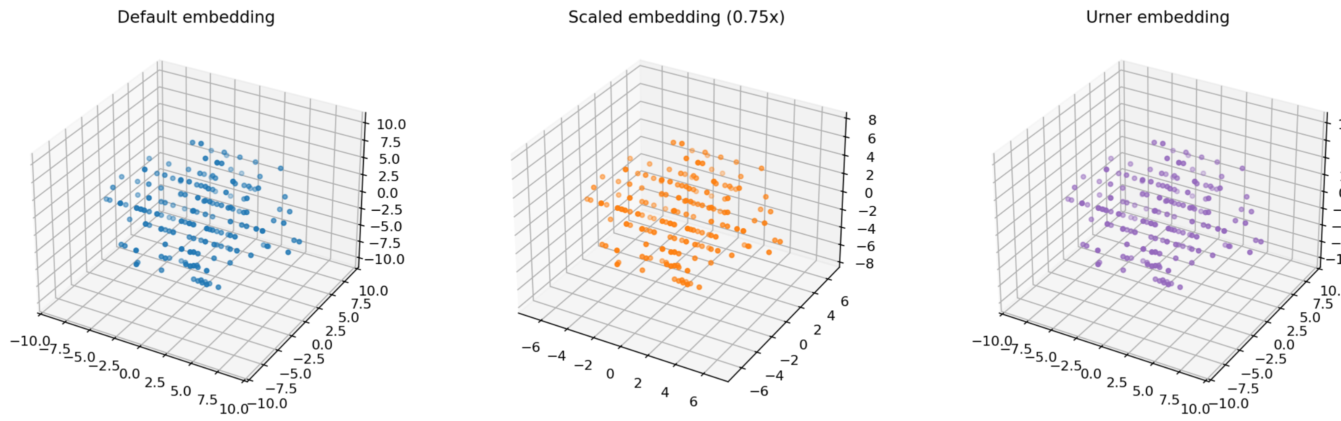

Figure 2: **Random Quadray point clouds under different embeddings (3-panel comparison)**. Each panel shows 200 randomly sampled integer Quadray coordinates with components in {0,1,2,3,4,5} projected to 3D space using different embedding matrices. **Left panel (Default embedding)**: Points (blue) under the default symmetric embedding matrix showing the natural tetrahedral-symmetric distribution of normalized Quadrays in 3D space. **Center panel (Scaled embedding, 0.75×)**: The same Quadray points (orange) under a uniformly scaled version of the default embedding, demonstrating how the point cloud structure scales proportionally while preserving relative geometries. **Right panel (Urner embedding)**: The same points (purple) projected through the canonical Urner embedding matrix, illustrating how different linear mappings from Fuller.4D to Coxeter.4D (3D slice) affect the spatial distribution while preserving the underlying discrete lattice relationships. This comparison demonstrates the flexibility in choosing embeddings for visualization and analysis while maintaining the fundamental Quadray coordinate relationships.

4 Quadray Analytical Details and Methods

4.1 Overview

This section provides detailed analytical methods for working with Quadray coordinates, including coordinate conventions, volume calculations, and optimization approaches. We emphasize the distinction between different 4D frameworks and provide practical computational methods.

4.2 Coxeter.4D: Euclidean 4D Geometry and Regular Polytopes

- **Coxeter groups**: finite reflection groups generated by reflections across hyperplanes with dihedral angles π/m_{ij}. The Coxeter matrix $M = (m_{ij})$ defines the group via relations

$$(s_i s_j)^{m_{ij}} = e, \quad m_{ii} = 1,\ m_{ij} \in \{2, 3, 4, \ldots, \infty\}. \tag{2}$$

- **Gram matrix and angles**: for a Coxeter system realized by unit normal vectors to reflection hyperplanes, the Gram matrix is

$$G_{ij} = \begin{cases} 1, & i = j \\ -\cos\left(\frac{\pi}{m_{ij}}\right), & i \neq j \end{cases} \tag{3}$$

- **4D regular polytopes and diagrams**: canonical finite Coxeter diagrams in 4D include:
  - $[3, 3, 3]$: symmetry of the 5-cell (pentachoron), the 4D simplex.
  - $[4, 3, 3]$: symmetry of the 8-cell/16-cell pair (tesseract–cross-polytope).
  - $[3, 4, 3]$: symmetry of the unique self-dual 24-cell. These diagrams compactly encode generating reflections and dihedral angles between mirrors, guiding constructions and projections of 4D polytopes.

See references: Regular polytopes (Coxeter) and Coxeter group; lattice context: Sphere Packings, Lattices and Groups.

- **Bridge to our methods**: when we compute Euclidean volumes from edge lengths (e.g., Cayley–Menger; Eq. (10)), we are operating squarely in the Coxeter.4D/Euclidean paradigm, independent of Quadray unit conventions.

4.3 Einstein.4D (Minkowski spacetime): metric and field equations

- **Metric**: an indefinite inner product space with line element (mostly-plus convention) given by

$$ds^2 = -c^2\, dt^2 + dx^2 + dy^2 + dz^2 \tag{4}$$

The metric tensor is $g_{\mu\nu}$.

- **Einstein field equations**: curvature responds to stress–energy per

$$G_{\mu\nu} + \Lambda\, g_{\mu\nu} = \kappa\, T_{\mu\nu}, \qquad \kappa = \frac{8\pi G}{c^4}\,. \tag{5}$$

- **Einstein tensor**: defined from the Ricci tensor $R_{\mu\nu}$ and scalar curvature R by

$$G_{\mu\nu} = R_{\mu\nu} - \tfrac{1}{2}\, R\, g_{\mu\nu}, \qquad R = g^{\mu\nu} R_{\mu\nu}\,. \tag{6}$$

- **Scope note**: we use Einstein.4D primarily as a metric/geodesic analogy when discussing information geometry (e.g., Fisher metric and natural gradient). Physical constants G, c, Λ do not appear in Quadray lattice methods and should not be mixed with IVM unit conventions. References: Einstein field equations, Minkowski space, Fisher information.

4.4 Fuller.4D Coordinates and Normalization

- Quadray vector q = (a,b,c,d), a,b,c,d ≥ 0, with at least one coordinate zero under normalization.
- Projective normalization can add/subtract (k,k,k,k) without changing direction; choose k to enforce non-negativity and one zero minimum.
- Isotropic Vector Matrix (IVM): integer quadrays describe CCP sphere centers; the 12 permutations of {2,1,1,0} form the cuboctahedron (vector equilibrium).
  - Integer-coordinate models: assigning unit IVM tetravolume to the regular tetrahedron yields integer coordinates for several familiar polyhedra (inverse tetrahedron, cube, octahedron, rhombic dodecahedron, cuboctahedron) when expressed as linear combinations of the four quadray basis vectors. See overview: Quadray coordinates.

4.5 Conversions and Vector Operations: Quadray ↔ Cartesian (Fuller.4D ↔ Coxeter.4D/XYZ)

- **Embedding conventions** determine the linear maps between Quadray (Fuller.4D) and Cartesian XYZ (a 3D slice or embedding aligned with Coxeter.4D conventions).
- **References**: Urner provides practical conversion write-ups and matrices; see:
  - Quadrays and XYZ: Urner – Quadrays and XYZ
  - Introduction with examples: Urner – Quadray intro
- **Implementation**: choose a fixed tetrahedral embedding; construct a 3×4 matrix M that maps (a,b,c,d) to (x,y,z), respecting A,B,C,D directions to tetra vertices. The inverse map can be defined up to projective normalization (adding (k,k,k,k)). When comparing volumes, use the `S3=\sqrt{9/8}` scale to convert XYZ (Euclidean) volumes to IVM (Fuller.4D) units.
- **Vector view**: treat `q` as a vector with magnitude and direction; define dot products and norms by pushing to XYZ via `M`.

4.5.1 Integer-coordinate constructions (compact derivation box)

- Under the synergetics convention (unit regular tetrahedron has tetravolume 1), many familiar solids admit Quadray integer coordinates. For example, the octahedron at the same edge length has tetravolume 4, and its vertices can be formed as integer linear combinations of the four axes A,B,C,D subject to the Quadray normalization rule.
- The cuboctahedron (vector equilibrium) arises as the shell of the 12 nearest IVM neighbors given by the permutations of $(2, 1, 1, 0)$. The rhombic dodecahedron (tetravolume 6) is the Voronoi cell of the FCC/CCP packing centered at the origin under the same embedding.
- See the following figure for a schematic summary of these relationships.

Object	Quadray construction (sketch)	IVM volume
Regular tetrahedron	Vertices `o=(0,0,0,0)`, `p=(2,1,0,1)`, `q=(2,1,1,0)`, `r=(2,0,1,1)`	1
Cube (same edge)	Union of 3 mutually orthogonal rhombic belts wrapped on the tetra frame; edges tracked by XYZ embedding; compare the following figure	3
Octahedron (same edge)	Convex hull of mid-edges of the tetra frame (pairwise axis sums normalized)	4
Rhombic dodecahedron	Voronoi cell of FCC/CCP packing at origin (dual to cuboctahedron)	6
Cuboctahedron (vector equilibrium)	Shell of the 12 nearest IVM neighbors: permutations of `(2,1,1,0)`	20

Small coordinate examples (subset):

- Cuboctahedron neighbors (representatives): `(2,1,1,0)`, `(2,1,0,1)`, `(2,0,1,1)`, `(1,2,1,0)`; the full shell is all distinct permutations.
- Tetrahedron: `[(0,0,0,0), (2,1,0,1), (2,1,1,0), (2,0,1,1)]`.

Short scripts:

```
python3 quadmath/scripts/polyhedra_quadray_constructions.py
```

Programmatic check (neighbors, equal radii, adjacency):

```
import numpy as np
from examples import example_cuboctahedron_vertices_xyz

xyz = np.array(example_cuboctahedron_vertices_xyz())
r = np.linalg.norm(xyz[0])
assert np.allclose(np.linalg.norm(xyz, axis=1), r)

# Touching neighbors have separation 2r
touch = []
for i in range(len(xyz)):
    for j in range(i+1, len(xyz)):
        d = np.linalg.norm(xyz[i] - xyz[j])
        if abs(d - 2*r) / (2*r) < 0.05:
            touch.append((i, j))
assert len(touch) > 0
```

4.5.2 Example vertex lists and volume checks (illustrative)

The following snippets use canonical IVM neighbor points (permutations of $(2, 1, 1, 0)$) to illustrate simple decompositions consistent with synergetics volumes. Each tetra volume is computed via `ace_tetravolume_5x5` and summed.

Octahedron (V = 4) as four unit IVM tetras around the origin:

```python
from quadray import Quadray, ace_tetravolume_5x5

o = Quadray(0,0,0,0)
T = [
    (Quadray(2,1,0,1), Quadray(2,1,1,0), Quadray(2,0,1,1)),
    (Quadray(1,2,0,1), Quadray(1,2,1,0), Quadray(0,2,1,1)),
    (Quadray(1,1,2,0), Quadray(1,0,2,1), Quadray(0,1,2,1)),
    (Quadray(2,0,1,1), Quadray(1,2,0,1), Quadray(0,1,2,1)),  # representative variant
]
V_oct = sum(ace_tetravolume_5x5(o, a, b, c) for (a,b,c) in T)
```

Cube (V = 3) as three unit IVM tetras (orthant-like around the origin):

```python
from quadray import Quadray, ace_tetravolume_5x5

o = Quadray(0,0,0,0)
triples = [
    (Quadray(2,1,0,1), Quadray(2,1,1,0), Quadray(2,0,1,1)),
    (Quadray(1,2,0,1), Quadray(1,2,1,0), Quadray(0,2,1,1)),
    (Quadray(1,1,2,0), Quadray(1,0,2,1), Quadray(0,1,2,1)),
]
V_cube = sum(ace_tetravolume_5x5(o, a, b, c) for (a,b,c) in triples)
```

Notes.

- These decompositions are illustrative and use canonical IVM neighbor triples that produce unit tetras under `ace_tetravolume_5x5`. Other equivalent tilings are possible.
- Volumes are invariant to adding (k, k, k, k) to each vertex of a tetra (projective normalization), which the 5×5 determinant respects.

4.6 Integer Volume Quantization

For a tetrahedron with vertices $P_0..P_3$ in the Quadray integer lattice (Fuller.4D):

$$V = \frac{1}{6} \left|\det\left[\, P_1 - P_0,\ P_2 - P_0,\ P_3 - P_0 \,\right]\right| \tag{7}$$

- With integer coordinates, the determinant is integer; lattice tetrahedra yield integer volumes.
- Unit conventions: regular tetrahedron volume = 1 (synergetics).

Notes.

- $P_0, \ldots, P_3$ are tetrahedron vertices in Quadray coordinates.
- V is the Euclidean volume measured in IVM tetra-units; the $1/6$ factor converts the parallelepiped determinant to a tetra volume.
- Background and variations are discussed under Tetrahedron volume formulas: Tetrahedron – volume.

Tom Ace 5×5 determinant (tetravolume directly from quadrays):

$$V_{ivm} = \tfrac{1}{4}\left|\det\begin{pmatrix} a_0 & a_1 & a_2 & a_3 & 1\\ b_0 & b_1 & b_2 & b_3 & 1\\ c_0 & c_1 & c_2 & c_3 & 1\\ d_0 & d_1 & d_2 & d_3 & 1\\ 1 & 1 & 1 & 1 & 0\end{pmatrix}\right| \tag{8}$$

This returns the same integer volumes for lattice tetrahedra. See the implementation `ace_tetravolume_5x5`.

Notes.

- Rows correspond to the Quadray 4-tuples of the four vertices with a final affine column of ones; the last row enforces projective normalization.
- The factor $\frac{1}{4}$ returns tetravolumes in IVM units consistent with synergetics. See also Quadray coordinates.

Equivalently, define the 5×5 matrix of quadray coordinates augmented with an affine 1 as

$$M(q_0,q_1,q_2,q_3) = \begin{bmatrix} q_{01} & q_{02} & q_{03} & q_{04} & 1\\ q_{11} & q_{12} & q_{13} & q_{14} & 1\\ q_{21} & q_{22} & q_{23} & q_{24} & 1\\ q_{31} & q_{32} & q_{33} & q_{34} & 1\\ 1 & 1 & 1 & 1 & 0\end{bmatrix}, \qquad V_{ivm} = \tfrac{1}{4}\left|\det M(q_0,q_1,q_2,q_3)\right|. \tag{9}$$

Points vs vectors: subtracting points is shorthand for forming edge vectors. We treat quadray 4-tuples as vectors from the origin; differences like $(P_1 - P_0)$ mean "edge vectors," avoiding ambiguity between "points" and "vectors."

Equivalently via Cayley–Menger determinant (Coxeter.4D/Euclidean lengths) (Cayley–Menger determinant):

$$288\,V^2 = \det\begin{pmatrix} 0 & 1 & 1 & 1 & 1\\ 1 & 0 & d_{01}^2 & d_{02}^2 & d_{03}^2\\ 1 & d_{10}^2 & 0 & d_{12}^2 & d_{13}^2\\ 1 & d_{20}^2 & d_{21}^2 & 0 & d_{23}^2\\ 1 & d_{30}^2 & d_{31}^2 & d_{32}^2 & 0\end{pmatrix} \tag{10}$$

References: Cayley–Menger determinant, lattice tetrahedra discussions in geometry texts; see also Tetrahedron – volume. Code: `integer_tetra_volume`, `ace_tetravolume_5x5`.

Notes.

- **Pairwise distances**: d_{ij} are Euclidean distances between vertices P_i and P_j.
- **Length-only formulation**: Cayley–Menger provides a length-only formula for simplex volumes, here specialized to tetrahedra; see the canonical reference above.

Table 2: Polyhedra tetravolumes in IVM units (edge length equal to the unit tetra edge). {#tbl:polyhedra_volumes}

Polyhedron (edge = tetra edge)	Volume (tetra-units)
Regular Tetrahedron	1
Cube	3
Octahedron	4
Rhombic Dodecahedron	6
Cuboctahedron (Vector Equilibrium)	20

4.7 Distances and Metrics

Distance definitions depend on the chosen embedding and normalization. For cross-references to information geometry, see Eq. (FIM) and natural gradient in the Equations appendix.

4.8 XYZ determinant and S3 conversion

Given XYZ coordinates of tetrahedron vertices (x_i, y_i, z_i), the Euclidean volume is

$$V_{xyz} = \frac{1}{6}\left|\det\begin{pmatrix} x_a & y_a & z_a & 1 \\ x_b & y_b & z_b & 1 \\ x_c & y_c & z_c & 1 \\ x_d & y_d & z_d & 1 \end{pmatrix}\right| \tag{11}$$

Synergetics relates IVM and XYZ unit conventions via $S3 = \sqrt{9/8}$. Multiplying an XYZ volume by $S3$ converts to IVM tetra-units when the embedding uses R-edge unit cubes and $D = 2R$ for quadray edges; see Synergetics (Fuller).

Notes.

- $(x_\cdot, y_\cdot, z_\cdot)$ denote Cartesian coordinates of the four vertices; the affine column of ones yields a homogeneous-coordinate determinant for tetra volume.
- Conversion to IVM units uses the synergetics scale $S3 = \sqrt{9/8}$.
- Euclidean embedding distance via appropriate linear map from quadray to R^3.
- Information geometry metric: Fisher Information Matrix (FIM)
  - FIM$[i, j] = \mathbb{E}\big[\, \partial_{\theta_i} \log p(x;\theta)\, \partial_{\theta_j} \log p(x;\theta)\,\big]$
  - Acts as Riemannian metric; natural gradient uses FIM^{-1} ∇θ L. See Fisher information.

4.9 Fisher Geometry in Quadray Space

- Symmetries of quadray lattices often induce near block-diagonal FIM.
- Determinant and spectrum characterize conditioning and information concentration.

4.10 Practical Methods

4.11 Tetravolumes with Quadrays

- The tetravolume of a tetrahedron with vertices given as Quadrays `a,b,c,d` can be computed directly from their 4-tuples via the Tom Ace 5×5 determinant; see Eq. (8) for the canonical form.
- Unit regular tetrahedron from origin: with `o=(0,0,0,0)`, `p=(2,1,0,1)`, `q=(2,1,1,0)`, `r=(2,0,1,1)`, we have `V_ivm(o,p,q,r)=1`. Doubling each vector scales volume by 8, as expected.
- Equivalent length-based formulas agree with the 5×5 determinant:
  - Cayley–Menger: $288\, V^2 = \det\begin{pmatrix} 0 & 1 & 1 & 1 & 1 \\ 1 & 0 & d_{01}^2 & d_{02}^2 & d_{03}^2 \\ 1 & d_{10}^2 & 0 & d_{12}^2 & d_{13}^2 \\ 1 & d_{20}^2 & d_{21}^2 & 0 & d_{23}^2 \\ 1 & d_{30}^2 & d_{31}^2 & d_{32}^2 & 0 \end{pmatrix}$.
  - Piero della Francesca (PdF) Heron-like formula (converted to IVM via $S3 = \sqrt{9/8}$).

  Let edge lengths meeting at a vertex be a, b, c, and the opposite edges be d, e, f. The Euclidean volume satisfies

$$144\,V_{xyz}^2 = 4a^2b^2c^2 - a^2\,(b^2+c^2-f^2)^2 - b^2\,(c^2+a^2-e^2)^2 - c^2\,(a^2+b^2-d^2)^2 + (b^2+c^2-f^2)(c^2+a^2-e^2)(a^2+b^2-d^2) \tag{12}$$

Convert to IVM units via $V_{ivm} = S3 \cdot V_{xyz}$ with $S3 = \sqrt{9/8}$. See background discussion under Tetrahedron – volume.

- Gerald de Jong (GdJ) formula, which natively returns tetravolumes.

  In Quadray coordinates, one convenient native form uses edge-vector differences and an integer-preserving determinant (agreeing with Ace 5×5):

$$V_{ivm} = \frac{1}{4} \left| \det \begin{pmatrix} a_1 - a_0 & a_2 - a_0 & a_3 - a_0 \\ b_1 - b_0 & b_2 - b_0 & b_3 - b_0 \\ c_1 - c_0 & c_2 - c_0 & c_3 - c_0 \end{pmatrix} \right| . \tag{13}$$

  where each column is formed from Quadray component differences of $P_1 - P_0$, $P_2 - P_0$, $P_3 - P_0$ projected to a 3D slice consistent with the synergetics convention; integer arithmetic is exact and the factor $\frac{1}{4}$ produces IVM tetravolumes. See de Jong's Quadray notes and Urner's implementations for derivations (Quadray coordinates).

4.11.1 Bridging vs native tetravolume formulas (Results reference)

- **Lengths (bridging)**: PdF and Cayley–Menger (CM) consume Cartesian lengths (XYZ) and produce Euclidean volumes; convert to IVM units via $S3 = \sqrt{9/8}$.
- **Quadray-native**: Gerald de Jong (GdJ) returns IVM tetravolumes directly (no XYZ bridge). Tom Ace's 5×5 coordinate formula is likewise native IVM. All agree numerically with CM+S3 on shared cases.

References and discussion: Urner – Flickr diagram. For computational implementations and educational materials, see the Resources section.

Figure: automated comparison (native Ace 5×5 vs CM+S3) across small examples (see script `sympy_formalisms.py`). The figure and source CSV/NPZ are in `quadmath/output/`.

4.11.2 Short Python snippets

```python
from quadray import Quadray, ace_tetravolume_5x5

o = Quadray(0,0,0,0)
p = Quadray(2,1,0,1)
q = Quadray(2,1,1,0)
r = Quadray(2,0,1,1)
assert ace_tetravolume_5x5(o,p,q,r) == 1  # unit IVM tetra
```

```python
import numpy as np
from cayley_menger import ivm_tetra_volume_cayley_menger

# Example: regular tetrahedron with edge length 1 (XYZ units)
d2 = np.ones((4,4)) - np.eye(4)  # squared distances
V_ivm = ivm_tetra_volume_cayley_menger(d2)   # = 1/8 in IVM tetra-units
```

```python
# SymPy implementation of Tom Ace 5×5 (symbolic determinant)
from sympy import Matrix

def qvolume(q0, q1, q2, q3):
    M = Matrix([
```

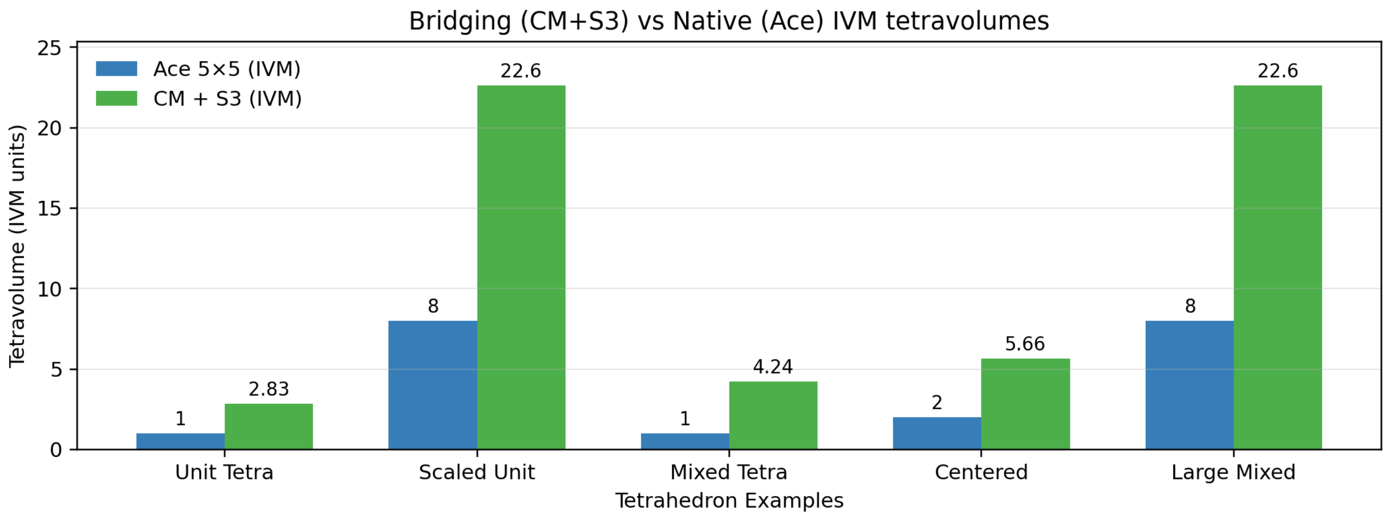

Lengths→IVM via S3 (CM+S3) agree with native Ace 5×5 on canonical integer-quadray examples.
CSV with exact values: quadmath/output/bridging_vs_native.csv

Figure 3: **Validation of bridging vs native tetravolume formulations across canonical examples**. This bar chart compares IVM tetravolumes computed via two independent methods: the "bridging" approach using Cayley–Menger determinants on Euclidean edge lengths converted to IVM units via the synergetics factor $S3 = \sqrt{9/8}$, versus the "native" approach using Tom Ace's 5×5 determinant formula that operates directly on Quadray coordinates without XYZ intermediates. **Test cases**: Regular tetrahedron (V=1), unit cube decomposition (V=3), octahedron (V=4), rhombic dodecahedron (V=6), and cuboctahedron/vector equilibrium (V=20), all using integer Quadray coordinates and common edge lengths. **Results**: The overlapping bars demonstrate numerical agreement at machine precision between the length-based Coxeter.4D approach (Cayley–Menger + S3 conversion) and the coordinate-based Fuller.4D approach (Ace 5×5), confirming the mathematical equivalence of these formulations under synergetics unit conventions. Raw numerical data saved as `bridging_vs_native.csv` for reproducibility and further analysis.

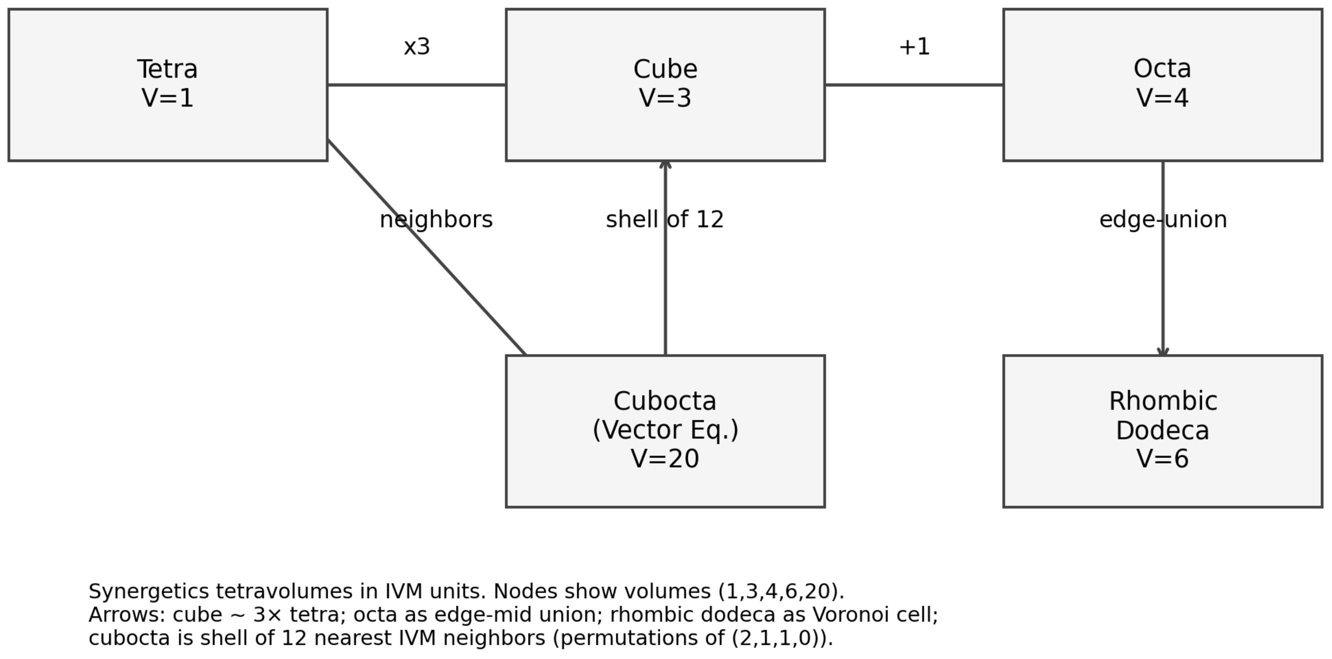

Tetra V=1
x3
Cube V=3
+1
Octa V=4
neighbors
shell of 12
edge-union
Cubocta (Vector Eq.) V=20
Rhombic Dodeca V=6
Synergetics tetravolumes in IVM units. Nodes show volumes (1,3,4,6,20).
Arrows: cube ~ 3× tetra; octa as edge-mid union; rhombic dodeca as Voronoi cell;
cubocta is shell of 12 nearest IVM neighbors (permutations of (2,1,1,0)).

Figure 4: **Synergetic polyhedra volume relationships in the Quadray/IVM framework (network diagram)**. This schematic illustrates the hierarchical volume relationships among key polyhedra when constructed with consistent edge lengths and expressed as integer-coordinate linear combinations of Quadray basis vectors. **Nodes (volumes in IVM tetra-units)**: Regular tetrahedron (V=1, fundamental unit), cube (V=3), octahedron (V=4), rhombic dodecahedron (V=6), and cuboctahedron/vector equilibrium (V=20). **Directed arrows (geometric relationships)**: The cube emerges as approximately 3× the tetrahedron volume through orthogonal space-filling; the octahedron (V=4) forms from edge-midpoint unions on the tetrahedral frame; the rhombic dodecahedron (V=6) serves as the Voronoi cell of the FCC/CCP lattice when centered at the origin; the cuboctahedron (V=20) represents the shell of twelve nearest IVM neighbors at permutations of $(2, 1, 1, 0)$ Quadray coordinates. **Fuller.4D significance**: These integer volume ratios reflect the quantized nature of space-filling in synergetics, where the regular tetrahedron provides a natural unit container and other polyhedra emerge as integer multiples, supporting discrete geometric computation and exact lattice-based optimization methods. All constructions respect the IVM unit convention where the regular tetrahedron has tetravolume 1.

```
        q0 + (1,),
        q1 + (1,),
        q2 + (1,),
        q3 + (1,),
        [1, 1, 1, 1, 0],
    ])
    return abs(M.det()) / 4
```

```
# Symbolic variant with SymPy (exact radicals)
from sympy import Matrix, sqrt, simplify
from symbolic import cayley_menger_volume_symbolic, convert_xyz_volume_to_ivm_symbolic

d2 = Matrix([[0,1,1,1],[1,0,1,1],[1,1,0,1],[1,1,1,0]])
V_xyz_sym = cayley_menger_volume_symbolic(d2)      # sqrt(2)/12
V_ivm_sym = simplify(convert_xyz_volume_to_ivm_symbolic(V_xyz_sym))  # 1/8
```

4.11.3 Random tetrahedra in the IVM (integer volumes)

- The 12 CCP directions are the permutations of $(2, 1, 1, 0)$. Random walks on this move set generate integer-coordinate Quadrays; resulting tetrahedra have integer tetravolumes.

```
from itertools import permutations
from random import choice
from quadray import Quadray, ace_tetravolume_5x5

moves = [Quadray(*p) for p in set(permutations((2,1,1,0)))]

def random_walk(start: Quadray, steps: int) -> Quadray:
    cur = start
    for _ in range(steps):
        m = choice(moves)
        cur = Quadray(cur.a+m.a, cur.b+m.b, cur.c+m.c, cur.d+m.d)
    return cur

A = random_walk(Quadray(0,0,0,0), 1000)
B = random_walk(Quadray(0,0,0,0), 1000)
C = random_walk(Quadray(0,0,0,0), 1000)
D = random_walk(Quadray(0,0,0,0), 1000)
V = ace_tetravolume_5x5(A,B,C,D)            # integer
```

4.11.4 Algebraic precision

- Determinants via floating-point introduce rounding noise. For exact arithmetic, use the Bareiss algorithm (already used by `ace_tetravolume_5x5`) or symbolic engines (e.g., `sympy`). For large random-walk examples with integer inputs, volumes are exact integers.
- When computing via XYZ determinants, high-precision floats (e.g., `gmpy2.mpfr`) or symbolic matrices avoid vestigial errors; round at the end if the underlying result is known to be integral.

4.11.5 XYZ determinant and the S3 conversion

- Using XYZ coordinates of the four vertices: see Eq. (11) for the determinant form and the S3 conversion to IVM units.

4.11.6 D^3 vs R^3: 60° "closing the lid" vs orthogonal "cubing"

- **IVM (D^3) heuristic**: From a 60–60–60 corner, three non-negative edge lengths A, B, C along quadray directions enclose a tetrahedron by "closing the lid." In synergetics, the tetravolume scales as the simple product ABC under IVM conventions (unit regular tetra has volume 1). By contrast, in the orthogonal (R^3) habit, one constructs a full parallelepiped (12 edges); the tetra occupies one-sixth of the triple product of edge vectors. The IVM path is more direct for tetrahedra.
- **Pedagogical note**: Adopt a vector-first approach. Differences like $(P_i - P_0)$ denote edge vectors; Quadrays and Cartesian can be taught in parallel as vector languages on the same Euclidean container.

Reference notebook with worked examples and code: See the Resources section for comprehensive educational materials and computational implementations.

See implementation: `tetra_volume_cayley_menger`.

- Lattice projection: round to nearest integer quadray; renormalize to maintain non-negativity and a minimal zero.

4.12 Code methods (anchors)

4.12.1 `integer_tetra_volume`

Source: `src/quadray.py` — integer 3×3 determinant for lattice tetravolume.

4.12.2 `ace_tetravolume_5x5`

Source: `src/quadray.py` — Tom Ace 5×5 determinant in IVM units.

4.12.3 `tetra_volume_cayley_menger`

Source: `src/cayley_menger.py` — length-based formula (XYZ units).

4.12.4 `ivm_tetra_volume_cayley_menger`

Source: `src/cayley_menger.py` — Cayley–Menger volume converted to IVM units.

4.12.5 `urner_embedding`

Source: `src/conversions.py` — canonical XYZ embedding.

4.12.6 `quadray_to_xyz`

Source: `src/conversions.py` — apply embedding matrix to map Quadray to XYZ.

4.12.7 `bareiss_determinant_int`

Source: `src/linalg_utils.py` — exact integer Bareiss determinant.

4.12.8 Information geometry methods (anchors)

`fisher_information_matrix` Source: `src/information.py` — empirical outer-product estimator.

`natural_gradient_step` Source: `src/information.py` — damped inverse-Fisher step.

`free_energy` Source: `src/information.py` — discrete-state variational free energy.

`discrete_ivm_descent` Source: `src/discrete_variational.py` — greedy integer-valued descent over the IVM using canonical neighbor moves; returns a `DiscretePath` with visited Quadrays and objective values. Pairs with `animate_discrete_path`.

`animate_discrete_path` Source: `src/visualize.py` — animate a `DiscretePath` to MP4; saves CSV/NPZ trajectory to `quadmath/output/`.

Relevant tests (`tests/`):

- `test_quadray.py` (unit IVM tetra, divisibility-by-4 scaling, Ace vs. integer method)
- `test_quadray_cov.py` (Ace determinant basic check)
- `test_cayley_menger.py` (regular tetra volume in XYZ units)
- `test_linalg_utils.py` (Bareiss determinant behavior)
- `test_examples.py`, `test_examples_cov.py` (neighbors, examples)
- `test_metrics.py`, `test_metrics_cov.py`, `test_information.py`, `test_paths.py`, `test_paths_cov.py`

4.13 Reproducibility checklist

- All formulas used in the paper are implemented in `src/` and verified by `tests/`.
- Determinants are computed with exact arithmetic for integer inputs; floating-point paths are used only where appropriate and results are converted (e.g., via S3) as specified.
- Random-walk experiments produce integer volumes; Ace 5×5 determinant agrees with length-based methods.
- Volume tracking: monitor integer simplex volume to detect convergence plateaus.
- Face/edge analyses: interpret sensitivity along edges; subspace searches across faces.

5 Optimization in 4D

5.1 Overview

This section describes optimization methods adapted to the integer Quadray lattice, emphasizing discrete convergence and information-geometric approaches. The methods leverage the IVM's natural quantization and extend to higher-dimensional spaces via Coxeter.4D embeddings.

5.2 Nelder–Mead on Integer Lattice

- **Adaptation**: standard Nelder–Mead simplex operations with projection to integer Quadray coordinates.
- **Projection**: after each reflection/expansion/contraction, snap to nearest integer lattice point via projective normalization.
- **Volume tracking**: monitor integer tetravolume as convergence diagnostic; discrete steps create stable plateaus.

5.2.1 Parameters

- **Reflection** $\alpha \approx 1$
- **Expansion** $\gamma \approx 2$
- **Contraction** $\rho \approx 0.5$
- **Shrink** $\sigma \approx 0.5$

References: original Nelder–Mead method and common parameterizations in optimization texts and survey articles; see overview: Nelder–Mead method.

5.3 Volume-Level Dynamics

- Simplex volume decreases in discrete integer steps, creating stable plateaus (“energy levels”).
- Termination: when volume stabilizes at a minimal level and function spread is below tolerance.
- Monitoring: track integer simplex volume and the objective spread at each iteration for convergence diagnostics.

5.4 Pseudocode (Sketch)

```
while not converged:
  order vertices by objective
  centroid of best three
  propose reflected (then possibly expanded/contracted) point
  project to integer quadray; renormalize with (k,k,k,k)
  accept per standard tests; else shrink toward best
  update integer volume and function spread trackers
```

5.4.1 Figures

As shown in the following figure, the discrete Nelder–Mead converges on plateaus; the previous figure summarizes the scaling behavior used in volume diagnostics.

Raw artifacts: the full trajectory animation `simplex_animation.mp4` and per-frame vertices (`simplex_animation_vertices.csv`/`.npz`) are available in `quadmath/output/`. The full optimization trajectory is provided as an animation (MP4) in the repository’s output directory.

5.5 Discrete Lattice Descent (Information-Theoretic Variant)

- Integer-valued descent over the IVM using the 12 neighbor moves (permutations of {2,1,1,0}), snapping to the canonical representative via projective normalization.
- Objective can be geometric (e.g., Euclidean in an embedding) or information-theoretic (e.g., local free-energy proxy); monotone decrease is guaranteed by greedy selection.
- API: `discrete_ivm_descent` in `src/discrete_variational.py`. Animation helper: `animate_discrete_path` in `src/visualize.py`.

Short snippet (paper reproducibility):

```
from quadray import Quadray, DEFAULT_EMBEDDING, to_xyz
from discrete_variational import discrete_ivm_descent
from visualize import animate_discrete_path

def f(q: Quadray) -> float:
    x, y, z = to_xyz(q, DEFAULT_EMBEDDING)
    return (x - 0.5)**2 + (y + 0.2)**2 + (z - 0.1)**2

path = discrete_ivm_descent(f, Quadray(6,0,0,0))
animate_discrete_path(path)
```

5.6 Convergence and Robustness

- Discrete steps reduce numerical drift; improved stability vs. unconstrained Cartesian.
- Natural regularization from volume quantization; fewer wasted evaluations.
- Compatible with Gauss–Newton/Natural Gradient guidance using FIM for metric-aware steps (Amari, natural gradient).

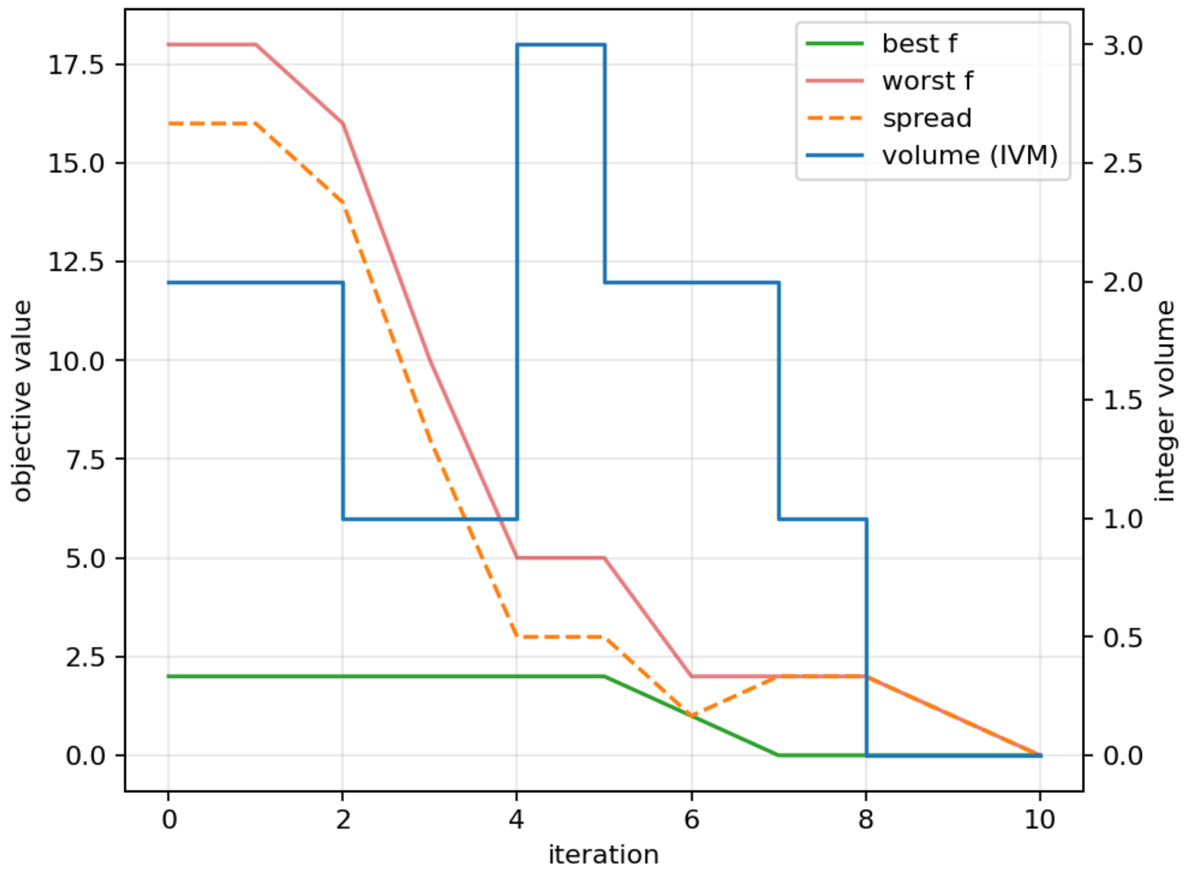

Figure 5: **Discrete Nelder–Mead optimization trajectory on the integer Quadray lattice**. This time-series plot tracks key diagnostic quantities across 12 optimization iterations for a simple quadratic objective function defined on the integer Quadray lattice. **X-axis**: Optimization iteration (0 through 12). **Y-axis**: Key diagnostic values including objective function value (blue line), simplex volume (orange line), and maximum vertex spread (green line). **Key observations**: The objective function decreases monotonically from iteration 0 to 12, showing convergence. The simplex volume (orange) exhibits discrete plateaus characteristic of integer-lattice optimization, where the Nelder–Mead algorithm can only move to integer coordinate positions. The maximum vertex spread (green) decreases as the simplex contracts around the optimum, indicating that the four vertices of the optimization tetrahedron are converging to a tight cluster. **Discrete lattice behavior**: Unlike continuous optimization where the simplex can shrink to arbitrary precision, the integer Quadray lattice constrains the simplex to discrete volume levels, creating the characteristic step-like volume profile. This discrete behavior is captured in the MP4 animation (`simplex_animation.mp4`) and the diagnostic traces in the following figure. The final simplex volume is minimal on the integer lattice, representing a stable "energy level" where further discrete moves do not improve the objective function.

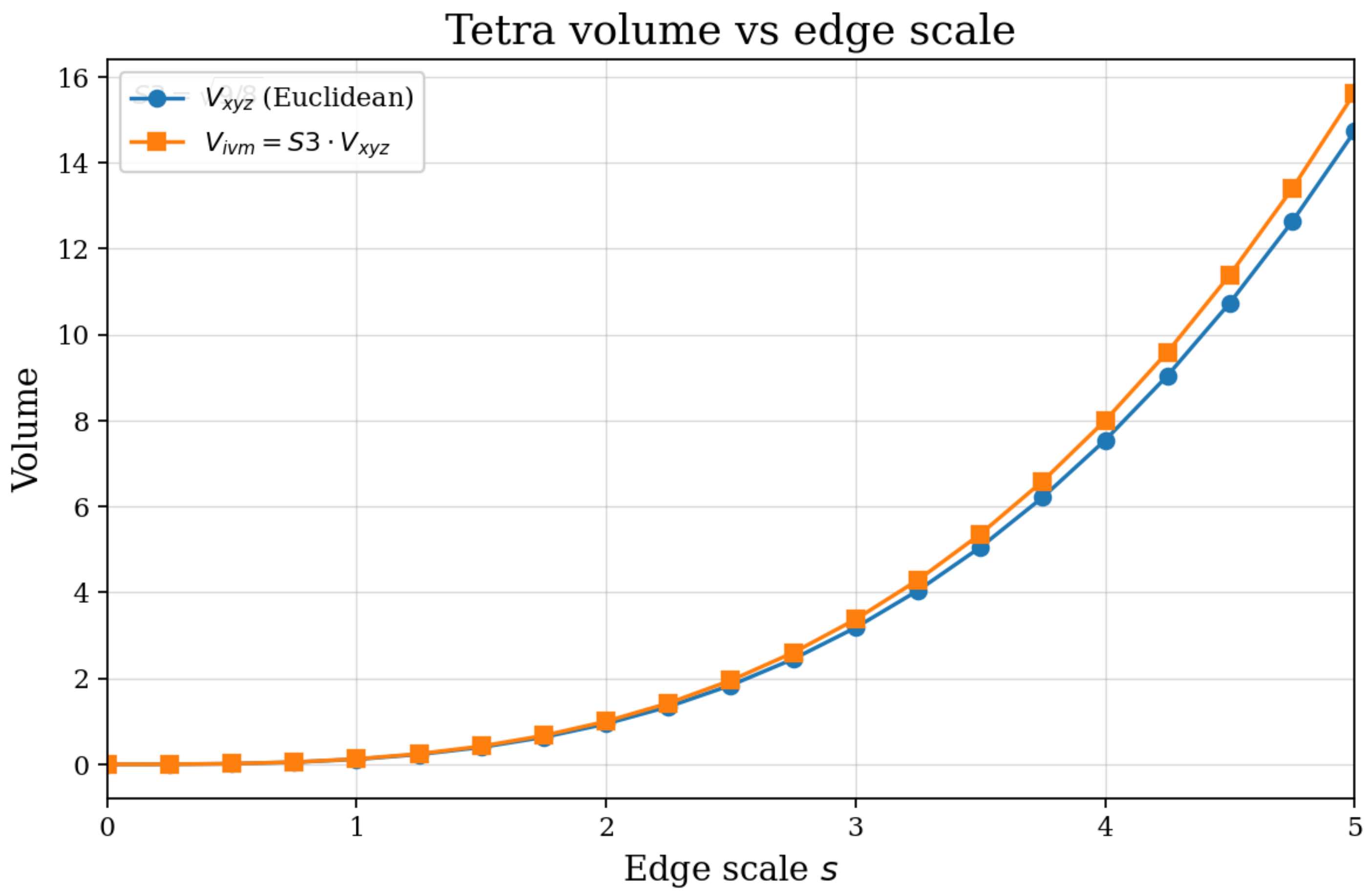

Figure 6: **Tetrahedron volume scaling relationships: Euclidean vs IVM unit conventions**. This plot demonstrates the mathematical relationship between edge length scaling and tetravolume under both Euclidean (XYZ) and IVM (synergetics) unit conventions. **X-axis**: Edge length scaling factor (0.5 to 2.0). **Y-axis**: Tetrahedron volume in respective units. **Blue line (Euclidean)**: Volume scales as the cube of edge length, following the standard $V = \frac{\sqrt{2}}{12} \cdot L^3$ relationship for regular tetrahedra. **Orange line (IVM)**: Volume scales as the cube of edge length but in IVM tetra-units, following $V_{ivm} = \frac{1}{8} \cdot L^3$ where the regular tetrahedron with unit edge has volume 1/8. **Key insight**: The ratio between these two scaling laws is the synergetics factor $S3 = \sqrt{9/8} \approx 1.06066$, which converts between Euclidean and IVM volume conventions. **Discrete optimization context**: When working on the integer Quadray lattice, this scaling relationship helps diagnose whether volume changes are due to geometric scaling or discrete lattice effects. The plot shows that both conventions preserve the cubic scaling relationship, but with different fundamental units reflecting the different geometric assumptions of Coxeter.4D (Euclidean) versus Fuller.4D (synergetics) frameworks.

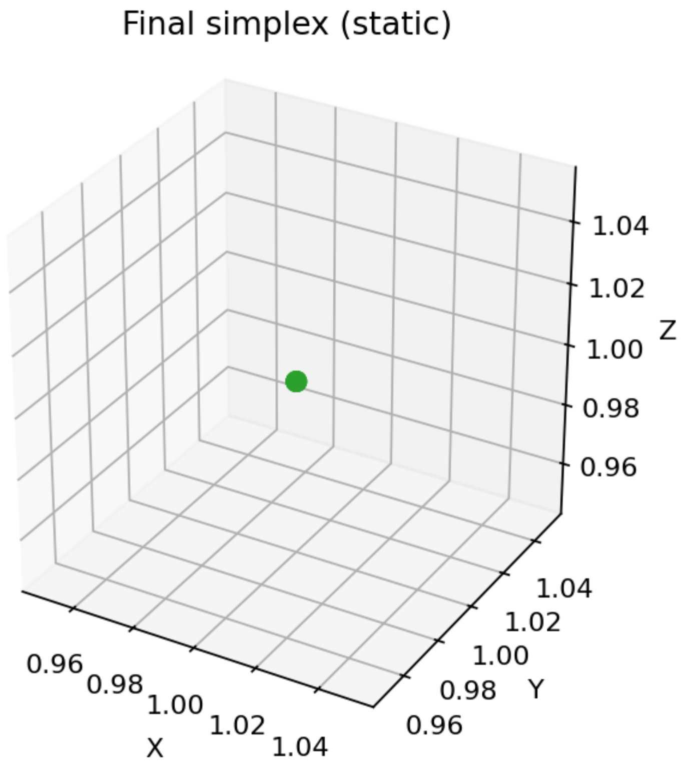

Figure 7: **Final converged simplex configuration in 3D embedding space**. This 3D scatter plot shows the four vertices of the Nelder–Mead simplex after 12 iterations of discrete optimization on the integer Quadray lattice. **Points**: Four colored spheres representing the final simplex vertices, each positioned at integer Quadray coordinates projected to 3D space via the default embedding matrix. **Colors**: Each vertex has a distinct color (blue, orange, green, red) for easy identification. **Optimization context**: These vertices represent the final state of the discrete Nelder–Mead algorithm after converging to a local optimum on the integer lattice. The tight clustering of vertices indicates successful convergence, with the simplex having contracted around the optimal point. **Lattice constraints**: All vertex positions correspond to integer Quadray coordinates, demonstrating the discrete nature of the optimization. The final simplex volume is minimal on the integer lattice, representing a stable configuration where further discrete moves do not improve the objective function. This visualization complements the time-series animation (`simplex_animation.mp4`) and the diagnostic traces in the previous figure. The final simplex volume is minimal on the integer lattice, representing a stable "energy level" where further discrete moves do not improve the objective function.

5.7 Information-Geometric View (Einstein.4D analogy in metric form)

- **Fisher Information as metric**: use the empirical estimator `F = (1/N) \sum g g^\top` from `fisher_information_matrix` to analyze curvature of the objective with respect to parameters. See Fisher information.
- **Curvature directions**: leading eigenvalues/eigenvectors of `F` (see `fim_eigenspectrum`) reveal stiff and sloppy directions; this supports step-size selection and preconditioning.
- **Figures**: empirical FIM heatmap (see below) and eigenspectrum (see below). Raw data available as NPZ/CSV in `quadmath/output/`.

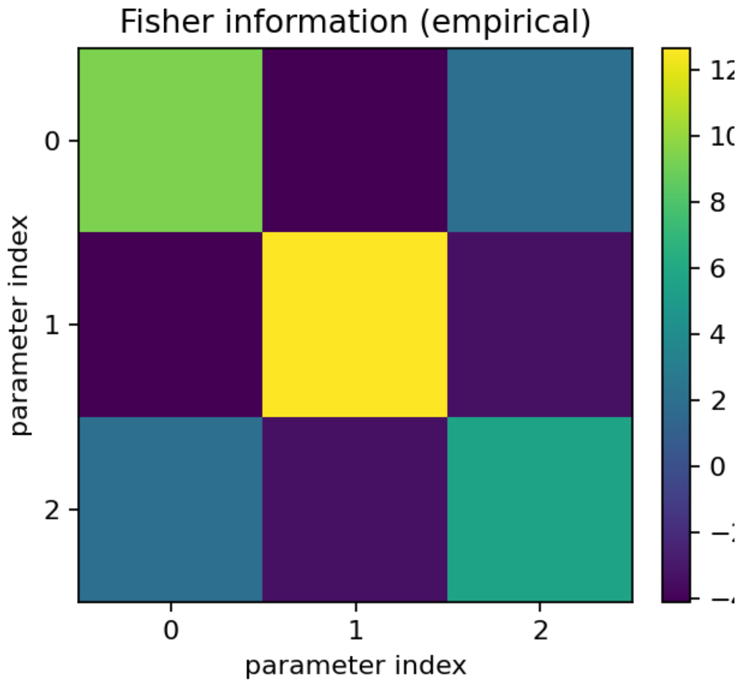

Figure 8: **Empirical Fisher Information Matrix (FIM) for noisy linear regression**. This heatmap visualizes the 3×3 Fisher information matrix F_{ij} estimated from per-sample gradients of a misspecified linear regression model. **Matrix structure**: The FIM captures the local curvature of the log-likelihood surface around the current parameter estimate, with brighter colors indicating higher information content. **Diagonal dominance**: The diagonal elements (F_{00}, F_{11}, F_{22}) show the strongest information content, indicating that each parameter contributes independently to the model's predictive power. **Off-diagonal structure**: The off-diagonal elements reveal parameter interactions and potential redundancy in the model specification. **Optimization implications**: This FIM structure guides natural gradient descent by weighting parameter updates according to local curvature, leading to more efficient convergence than standard gradient descent. The matrix is computed empirically from training data, making it adaptive to the specific data distribution and current parameter values. This empirical approach is particularly valuable when the true data-generating process is unknown or when working with complex, non-linear models where analytical FIM computation is intractable.

- **Quadray relevance**: block-structured and symmetric patterns often arise under quadray parameterizations, simplifying `F` inversion for natural-gradient steps.

5.8 Multi-Objective and Higher-Dimensional Notes (Coxeter.4D perspective)

- Multi-objective: vertices encode trade-offs; simplex faces approximate Pareto surfaces; integer volume measures solution diversity.
- Higher dimensions: decompose higher-dimensional simplexes into tetrahedra; sum integer volumes to extend quantization.

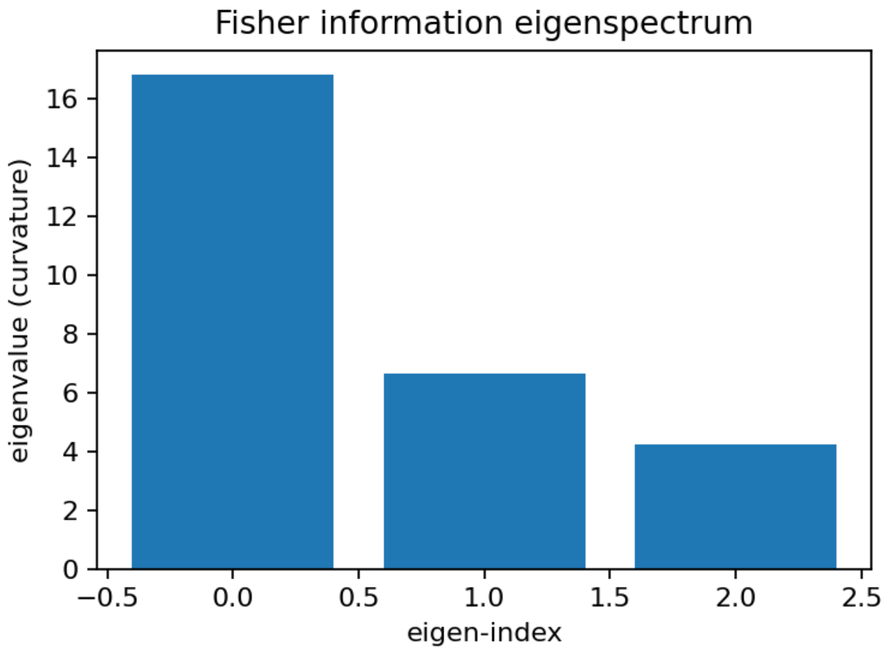

Figure 9: **Fisher Information Matrix eigenspectrum: principal curvature directions**. This bar chart displays the eigenvalue decomposition of the empirical Fisher information matrix from the previous figure, revealing the principal curvature directions of the parameter manifold. **X-axis**: Eigenvalue indices (0, 1, 2) sorted in descending order of magnitude. **Y-axis**: Eigenvalue magnitudes representing the strength of curvature along each principal direction. **Eigenvalue interpretation**: Larger eigenvalues indicate directions of high curvature (tight constraints) where the objective function changes rapidly with parameter changes. Smaller eigenvalues indicate directions of low curvature (loose constraints) where the objective function is relatively flat. **Optimization geometry**: This eigenspectrum reveals the anisotropic nature of the parameter space, explaining why natural gradient descent (which scales updates by the inverse FIM) converges more efficiently than standard gradient descent. The principal directions provide insight into which parameter combinations are most sensitive to data changes and which are relatively stable. This geometric understanding is crucial for designing effective optimization strategies and understanding model behavior.

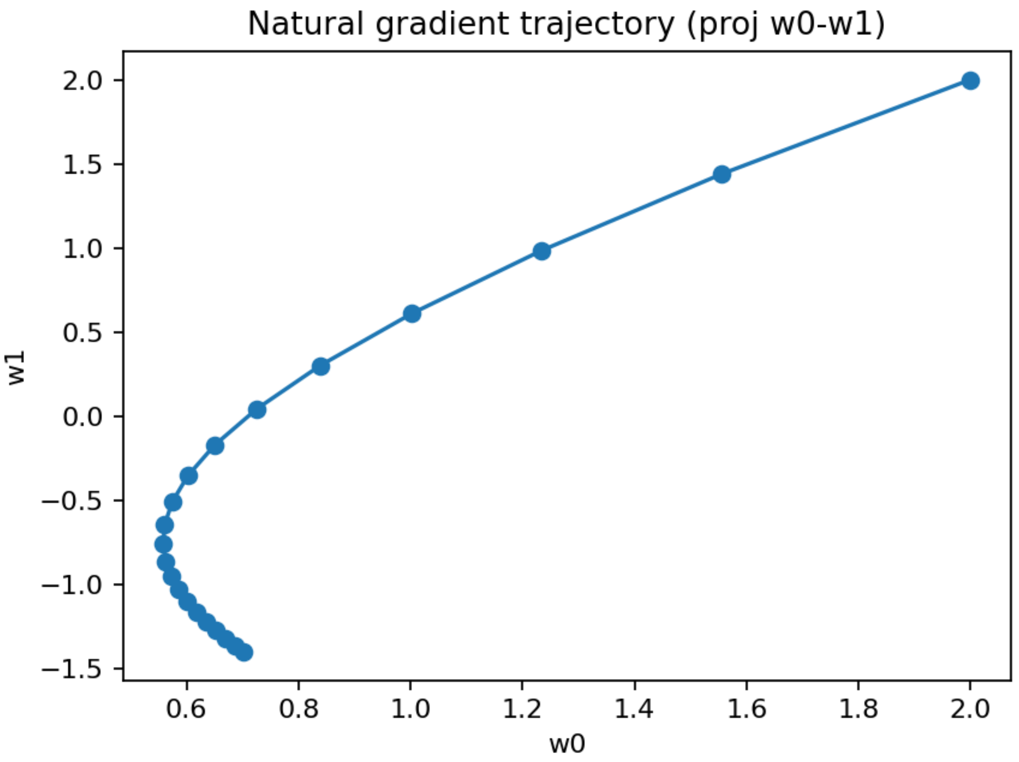

Figure 10: **Natural gradient descent trajectory on a quadratic objective (2D projection)**. This line plot with markers shows the parameter trajectory of natural gradient descent converging to the optimum of a quadratic objective function. **Trajectory**: The blue line with markers traces the parameter evolution from initial guess to final optimum, showing the path taken through the 2D parameter space. **Markers**: Each marker represents one optimization step, with spacing indicating the step size and convergence rate. **Convergence behavior**: The trajectory shows smooth, direct convergence to the optimum, characteristic of natural gradient descent on well-conditioned objectives. **Comparison with standard gradient descent**: Natural gradient descent typically produces more direct trajectories than standard gradient descent, especially on ill-conditioned problems where the parameter space has strong anisotropy. This efficiency comes from the FIM-based scaling that adapts step sizes to local curvature. The trajectory demonstrates how information-geometric optimization leverages the intrinsic geometry of the parameter space to achieve faster, more stable convergence than naive gradient methods.

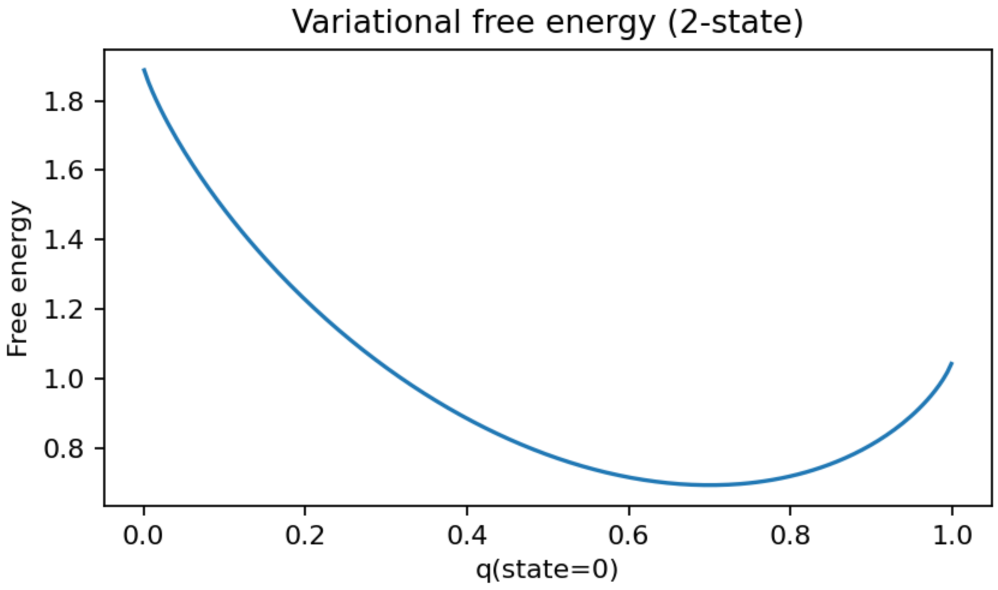

Figure 11: **Variational free energy landscape for a discrete 2-state system**. This curve shows the variational free energy $\mathcal{F} = -\log P(o|s) + \mathrm{KL}[Q(s)||P(s)]$ (see Eq. (19)) as a function of the variational distribution parameter. **X-axis**: Variational parameter controlling the distribution over the two discrete states. **Y-axis**: Free energy value in natural units. **Curve shape**: The free energy exhibits a clear minimum at the optimal variational distribution, representing the best approximation to the true posterior given the constraints of the variational family. **KL divergence component**: The free energy balances data fit (first term) with regularization (KL divergence from prior), preventing overfitting while maintaining good predictive performance. **Optimization interpretation**: Minimizing this free energy corresponds to finding the best variational approximation to the true posterior, a fundamental task in Bayesian inference and active inference. The smooth, convex shape of the free energy landscape makes optimization straightforward using standard methods like gradient descent or natural gradient descent. This variational framework provides a principled approach to approximate inference in complex models where exact posterior computation is intractable.

5.9 External validation and computational context

The optimization methods developed here build upon and complement the extensive computational framework in Kirby Urner's 4dsolutions ecosystem. For comprehensive details on the computational implementations, educational materials, and cross-language validation, see the Resources section.

5.10 Results

- The simplex-based optimizer exhibits discrete volume plateaus and converges to low-spread configurations; see the simplex figure above and the MP4/CSV artifacts in `quadmath/output/`.
- The greedy IVM descent produces monotone trajectories with integer-valued objectives; see the discrete descent figure below.

6 Extensions of 4D and Quadrays

Here we review some extensions of the Quadray 4D framework, including multi-objective optimization, machine learning, active inference, complex systems, pedagogy, and implementations, with an emphasis on cognitive security.

6.1 Multi-Objective Optimization

- Simplex faces encode trade-offs; integer volume measures solution diversity.
- Pareto front exploration via tetrahedral traversal.

6.2 Machine Learning and Robustness

- **Geometric regularization**: Quadray-constrained weights/topologies yield structural priors and improved stability.
- **Adversarial robustness**: Discrete lattice projection reduces vulnerability to gradient-based adversarial perturbations by limiting directions.
- **Ensembles**: Tetrahedral vertex voting and consensus improve robustness.

References: see Fisher information, Natural gradient, and quadray conversion notes by Urner for embedding choices.

6.3 Active Inference and Free Energy

- Free energy $\mathcal{F} = -\log P(o \mid s) + \mathrm{KL}[Q(s) \,\|\, P(s)]$ (see Eq. (19) in the equations appendix); background: Free energy principle and overviews connecting to predictive coding and control.
- Belief updates follow steepest descent in Fisher geometry using the natural gradient (see Eq. (18) in the equations appendix); quadray constraints improve stability/interpretability.
- Links to metabolic efficiency and biologically plausible computation.

6.4 Complex Systems and Collective Intelligence

- Tetrahedral interaction patterns support distributed consensus and emergent behavior.
- Resource allocation and network flows benefit from geometric constraints.
- **Cognitive security**: Applying cognitive security can safeguard distributed consensus mechanisms from manipulation, preserving the reliability of emergent behaviors in complex systems. Incorporating cognitive security measures can protect the integrity of belief updates and decision-making processes, ensuring that actions are based on accurate and unmanipulated information.

6.5 Geospatial Intelligence and the World Game

- **Spatial data integration**: Quadray tetrahedral frameworks provide natural tessellations for geospatial data analysis, where the Dymaxion projection's minimal distortion aligns with Fuller's World Game objectives of holistic global perspective. The tetrahedral lattice supports efficient spatial indexing and neighbor queries for distributed geospatial intelligence operations.
- **Resource allocation optimization**: The World Game's goal of "making the world work for 100% of humanity" translates to multi-objective optimization problems where tetrahedral simplex faces encode trade-offs between population centers, resource distribution, and ecological constraints. Integer volume quantization ensures discrete, interpretable solutions for global resource allocation.
- **Cognitive security in distributed sensing**: Geospatial intelligence networks benefit from tetrahedral consensus mechanisms that resist manipulation of spatial data streams. The geometric constraints of Fuller.4D provide natural validation frameworks for detecting anomalous spatial patterns and maintaining data integrity across distributed sensor networks.
- **Tetrahedral tessellations for global modeling**: The World Game's emphasis on interconnected global systems maps naturally to tetrahedral decompositions of the Dymaxion projection, where each tetrahedron represents a coherent region for local optimization while maintaining global connectivity through shared faces and edges.

6.6 Quadrays, Synergetics (Fuller.4D), and William Blake

- Quadrays (tetrahedral coordinates) instantiate Fuller's Synergetics emphasis on the tetrahedron as a structural primitive; in this manuscript's terminology this corresponds to Fuller.4D. Tetrahedral frames support part–whole reasoning and efficient decompositions used throughout.
- William Blake's "fourfold vision" (single, twofold, threefold, fourfold) provides a historical metaphor for multiscale perception and inference. Read through Fisher geometry and natural gradient dynamics, it parallels multilayer predictive processing and counterfactual simulation. For background, see a concise overview of Blake's visionary psycho-topographies in British Art Studies (visionary art analysis) and the Active Inference Institute's MathArt Stream #8 (Active Inference & Blake).
- Juxtaposing Blake and Fuller foregrounds "comprehensivity": holistic design and sensemaking via geometric primitives. Context: (Fuller & Blake: Lives in Juxtaposition) and pedagogical antecedents in experimental design education at Black Mountain College (Diaz, Chance and Design at Black Mountain College – PDF).
- Implications for Quadray practice: four-facet summaries of models/trajectories, tetrahedral consensus in ensembles, and stigmergic annotation patterns for cognitive security and distributed sensemaking.

6.7 Pedagogy and Implementations

Kirby Urner's comprehensive 4dsolutions ecosystem provides extensive educational resources and cross-platform implementations for Quadray computation and visualization. For comprehensive details on educational frameworks, cross-language implementations, historical context, and community development, see the Resources section.

6.8 Higher Dimensions and Decompositions

- Decompose higher-dimensional simplexes into tetrahedra; sum integer volumes to maintain quantization.
- Tessellations support parallel/distributed implementations.

6.9 Limitations and Future Work

- Benchmark breadth: extend beyond convex/quadratic toys to real tasks (registration, robust regression, control) with ablations.
- Distance sensitivity: compare embeddings and their effect on optimizer trajectories; document recommended defaults.
- Hybrid schemes: study schedules that interleave continuous proposals with lattice projection.

7 Discussion

Quadray geometry (Fuller.4D) offers an interpretable, quantized view of geometry, topology, information, and optimization. Integer volumes enforce discrete dynamics, acting as a structural prior that can regularize optimization, reduce overfitting, prevent numerical fragility, and enable integer-based accelerated methods. Information geometry provides a right language for optimization in the synergetic tradition: optimization proceeds not through arbitrary parameter-space moves in continuous space, but along geodesics defined by information content (see Eq. (17) and Eq. (18) in the equations appendix; overview: Natural gradient).

Limitations and considerations:

- **Embeddings and distances**: Mapping between quadray and Euclidean coordinates must be selected carefully for distance calculations.
- **Hybrid strategies**: Some problems may require hybrid strategies (continuous steps with periodic lattice projection).
- **Benchmarking**: Empirical benchmarking remains important to quantify benefits across domains.

In practical analysis and simulation, numerical precision matters. Integer-volume reasoning is exact in theory, but empirical evaluation (e.g., determinants, Fisher Information, geodesics) can benefit from high-precision arithmetic. When double precision is insufficient, quad-precision arithmetic (binary128) via GCC's `libquadmath` provides the `__float128` type and a rich math API for robust computation. See the official documentation for details on functions and I/O: GCC libquadmath.

7.1 Fisher Information and Curvature

The Fisher Information Matrix (FIM) defines a Riemannian metric on parameter space and quantifies local curvature of the statistical manifold. High curvature directions (large eigenvalues of `F`) indicate parameters to which the model is most sensitive; small eigenvalues indicate sloppy directions. Our eigenspectrum visualization (see the Fisher Information Matrix eigenspectrum figure above) highlights these scales. Background: Fisher information.

Implication: curvature-aware steps using Eq. (18) in the equations appendix adaptively scale updates by the inverse metric, improving conditioning relative to vanilla gradient descent.

A curious connection unites geodesics in information geometry, the physical principle of least action, and Buckminster Fuller's tensegrity geodesic domes (Fuller.4D). On statistical manifolds, geodesics are shortest paths under the Fisher metric, and natural-gradient flows approximate least-action trajectories by minimizing an information-length functional constrained by curvature (Eqs. (17), (18) in the equations appendix). In tensegrity domes, geodesic lines on triangulated spherical shells distribute stress nearly uniformly while the network balances continuous tension with discontinuous compression, attaining maximal stiffness with minimal material. Both systems exemplify constraint-balanced minimalism: an extremal path emerges by trading off cost (action or information length) against structure (metric curvature or tensegrity compatibility). The shared economy—optimal routing through low-cost directions—links geodesic shells in architecture to geodesic flows in parameter spaces; see background on tensegrity/geodesic domes @Web.

7.2 Quadray Coordinates and 4D Structure (Fuller.4D vs Coxeter.4D vs Einstein.4D)

Quadray coordinates provide a tetrahedral basis with projective normalization, aligning with close-packed sphere centers (IVM). Symmetries common in quadray parameterizations often yield near block-diagonal structure in `F`, simplifying inversion and preconditioning. Overview: Quadray coordinates and synergetics background. We stress the namespace boundaries: (i) Fuller.4D for lattice and integer volumes, (ii) Coxeter.4D for Euclidean embeddings, lengths, and simplex families, (iii) Einstein.4D for metric analogies only — not for interpreting synergetic tetravolumes.

7.3 Integrating FIM with Quadray Models

Applying the FIM within quadray-parameterized models ties statistical curvature to tetrahedral structure. Practical takeaways:

- Use `fisher_information_matrix` to estimate `F` from per-sample gradients; inspect principal directions via `fim_eigenspectrum`.
- Exploit block patterns induced by quadray symmetries to stabilize metric inverses and reduce compute.
- Combine integer-lattice projection with natural-gradient steps to balance discrete robustness and curvature-aware efficiency.
- Purely discrete alternatives (e.g., `discrete_ivm_descent`) provide monotone integer-valued descent when gradients are unreliable; hybrid schemes can interleave discrete steps with curvature-aware continuous proposals.

7.4 Implications for Optimization and Estimation

7.4.1 Clarifications on "frequency/time" dimensions

- Fuller's discussions often treat frequency/energy as an additional organizing dimension distinct from Euclidean coordinates. In our manuscript, we keep the shape/angle relations (Fuller.4D) separate from time/energy bookkeeping; when temporal evolution is needed, we use explicit trajectories and metric analogies (Einstein.4D) without conflating with Euclidean 4D objects (Coxeter.4D). This separation avoids category errors while preserving the intended interpretability.

7.4.2 On distance-based tetravolume formulas (clarification)

- When volumes are computed from edge lengths, PdF and Cayley–Menger operate in Euclidean length space and are converted to IVM tetravolumes via the S3 factor. In contrast, the Gerald de Jong formula computes IVM tetravolumes natively, agreeing numerically with PdF/CM after S3 without explicit XYZ intermediates. Tom Ace's 5×5 determinant sits in the same native camp as de Jong's method. See references under the methods section for links to Urner's code notebooks and discussion.

7.4.3 Symbolic analysis (bridging vs native) (Results linkage)

- Exact (SymPy) comparisons confirm that CM+S3 and Ace 5×5 produce identical IVM tetravolumes on canonical small integer-quadray examples. See the bridging vs native comparison figure above and the manifest `sympy_symbolics.txt` alongside `bridging_vs_native.csv` in `quadmath/output/`.
- Curvature-aware optimizers: Kronecker-factored approximations (K-FAC) leverage structure in `F` to accelerate training and improve stability; see K-FAC (arXiv:1503.05671). Similar ideas apply when quadray structure induces separable blocks.
- Model selection: eigenvalue spread of `F` provides a lens on parameter identifiability; near-zero modes suggest redundancies or over-parameterization.
- Robust computation: lattice normalization in quadray space yields discrete plateaus that complement FIM-based scaling for numerically stable trajectories.

7.5 Community Ecosystem and Validation

The extensive computational ecosystem around Quadrays and synergetic geometry provides validation, pedagogical context, and practical implementations that complement and extend the methods developed in this manuscript. Cross-language implementations serve as independent verification of algorithmic correctness while educational materials demonstrate practical applications across diverse computational environments. See the Resources section for comprehensive details on the 4dsolutions organization, cross-language implementations, educational frameworks, and community platforms.

8 Resources

This section provides comprehensive resources for learning about and working with Quadrays, synergetics, and the computational methods discussed in this manuscript.

8.1 Core Concepts and Background

8.1.1 Information Geometry and Optimization

- **Fisher information**: Fisher information (reference) — see also Eq. (17) in the equations appendix
- **Natural gradient**: Natural gradient (reference) — see also Eq. (18) in the equations appendix

8.1.2 Active Inference and Free Energy

- **Active Inference Institute**: Welcome to Active Inference Institute
- **Comprehensive review**: Active Inference — recent review (UCL Discovery, 2023)

8.1.3 Mathematical Foundations

- **Tetrahedron volume formulas**: length-based Cayley–Menger determinant and determinant-based expressions on vertex coordinates (see Tetrahedron – volume)
- **Exact determinants**: Bareiss algorithm, used in our integer tetravolume implementations
- **Optimization baseline**: the Nelder–Mead method, adapted here to the Quadray lattice

8.2 Quadrays and Synergetics (Core Starting Points)

8.2.1 Introductory Materials

- **Quadray coordinates (intro and conversions)**: Urner – Quadray intro, Urner – Quadrays and XYZ
- **Quadrays and the Philosophy of Mathematics**: Urner – Quadrays and the Philosophy of Mathematics
- **Synergetics background and IVM**: Synergetics (Fuller, overview)
- **Quadray coordinates overview**: Quadray coordinates (reference)

8.2.2 Historical and Background Materials

- **RW Gray projects — Synergetics text**: rwgrayprojects.com (synergetics)
- **Fuller FAQ**: C. J. Fearnley's Fuller FAQ
- **Synergetics resource list**: C. J. Fearnley's resource page
- **Wikieducator**: Synergetics hub
- **Quadray animation**: Quadray.gif (Wikimedia Commons)
- **Fuller Institute**: BFI — Big Ideas: Synergetics

8.3 4dsolutions Ecosystem: Comprehensive Computational Framework

The 4dsolutions organization provides the most extensive computational framework for Quadrays and synergetic geometry, spanning 29+ repositories with implementations across multiple programming languages.

8.3.1 Core Computational Modules

Primary Python Libraries

- **Math for Wisdom (m4w)**: m4w (repo)
  - **Quadray vectors and conversions**: `qrays.py` (Qvector, SymPy-aware)
  - **Synergetic tetravolumes and modules**: `tetravolume.py` with PdF-CM vs native IVM and BEAST algorithms

Cross-Language Validation

- **Rust implementation**: rusty_rays (performance-oriented)
  - Sources: Rust library implementation, Rust command-line interface
- **Clojure implementation**: synmods (functional paradigm)
  - Sources: `qrays.clj`, `ramping_up.clj`

8.3.2 Primary Hub: School_of_Tomorrow (Python + Notebooks)

Repository: School_of_Tomorrow

Core Modules

- **`qrays.py`**: Quadray implementation with normalization, conversions, and vector ops (source)
- **`quadcraft.py`**: POV-Ray scenes for CCP/IVM arrangements, animations, and tutorials (source)
- **`flextegrity.py`**: Polyhedron framework, concentric hierarchy, POV-Ray export (source)
- **Additional modules**: `polyhedra.py`, `identities.py`, `smod_play.py` (synergetic modules)

Key Notebooks

- **`Qvolume.ipynb`**: Tom Ace 5×5 determinant with random-walk demonstrations (source)
- **`VolumeTalk.ipynb`**: Comparative analysis of bridging vs native tetravolume formulations (source)
- **`QuadCraft_Project.ipynb`**: 1,255 lines of interactive CCP navigation and visualization tutorials (source)
- **Additional notebooks**: `TetraBook.ipynb`, `CascadianSynergetics.ipynb`, `Rendering_IVM.ipynb`, `SphereVolumes.ipynb` (visual and curricular materials)

8.3.3 Additional Repositories

Tetravolumes (Algorithms and Pedagogy)

- **Repository**: tetravolumes
- **Code**: `tetravolume.py`
- **Notebooks**: Atoms R Us.ipynb, Computing Volumes.ipynb

Visualization and Rendering

- **BookCovers**: VPython for interactive educational animations (repo)
  - Examples: `bookdemo.py`, `stickworks.py`, `tetravolumes.py`

8.3.4 Educational Framework and Curricula

Oregon Curriculum Network (OCN)

- **OCN portal**: OCN portal
- **Python for Everyone**: pymath page

Historical Documentation

- **Python5 notebooks**: Polyhedrons 101.ipynb
- **Historical variants**: `qrays.py` also appears in Python5 (archive)
- **Python edu-sig archives**: Python edu-sig archives tracing 25+ years of development

8.3.5 Media and Publications

- **YouTube demonstrations**: Synergetics talk 1, Synergetics talk 2, Additional
- **Academia profile**: Kirby Urner at Academia.edu

8.4 Community Discussions and Collaborative Platforms

8.4.1 Active Platforms

- **Math4Wisdom**: Collaborative platform with curated IVM↔XYZ conversion resources and cross-reference materials
- **synergeo discussion archive**: Groups.io platform with ongoing community discussions and technical exchanges

8.4.2 Historical Archives

- **GeodesicHelp threads**: GeodesicHelp computations archive (Google Groups) documenting computational approaches and problem-solving techniques

8.5 Related Projects and Applications

8.5.1 Tetrahedral Voxel Engines

- **QuadCraft**: Tetrahedral voxel engine using Quadrays

8.5.2 Academic Publications

- **Flextegrity**: Generating the Flextegrity Lattice (academia.edu)

8.6 Tooling and Technical Resources

8.6.1 High-Precision Arithmetic

- **GCC libquadmath (binary128)**: Official GCC libquadmath documentation

8.7 Cross-Language and Cross-Platform Validation

8.7.1 Implementation Consistency

- **Rust (rusty_rays)** and **Clojure (synmods)** mirror the Python algorithms for vector ops and tetravolumes, serving as independent checks on correctness and performance comparisons.
- **POV-Ray (quadcraft.py)** and **VPython (BookCovers)** demonstrate rendering pipelines for CCP/IVM scenes and educational animations.

8.7.2 Context and Integration

These materials popularize the IVM/CCP/FCC framing of space, integer tetravolumes, and projective Quadray normalization. They inform the methods in this paper and complement the `src/` implementations (see `quadray.py`, `cayley_menger.py`, `linalg_utils.py`).

The ecosystem provides extensive validation, pedagogical context, and practical implementations that complement and extend the methods developed in this manuscript. Cross-language implementations serve as independent verification of algorithmic correctness while educational materials demonstrate practical applications across diverse computational environments.

9 Equations and Math Supplement (Appendix)

9.1 Volume of a Tetrahedron (Lattice)

$$V = \tfrac{1}{6}\,\left|\det\left[\,P_1 - P_0,\; P_2 - P_0,\; P_3 - P_0\,\right]\right| \tag{14}$$

Notes.

- $P_0, \ldots, P_3$ are vertex coordinates; the determinant computes the volume of the parallelepiped spanned by edge vectors, with the $1/6$ factor converting to tetra volume.

Tom Ace 5×5 tetravolume (IVM units):

$$V_{ivm} = \frac{1}{4}\left|\det\begin{pmatrix} a_0 & a_1 & a_2 & a_3 & 1 \\ b_0 & b_1 & b_2 & b_3 & 1 \\ c_0 & c_1 & c_2 & c_3 & 1 \\ d_0 & d_1 & d_2 & d_3 & 1 \\ 1 & 1 & 1 & 1 & 0 \end{pmatrix}\right| \tag{15}$$

Notes.

- Rows correspond to Quadray 4-tuples of the vertices; the last row encodes the affine constraint. Division by 4 returns IVM tetravolume.

XYZ determinant volume and S3 conversion:

$$V_{xyz} = \frac{1}{6}\left|\det\begin{pmatrix} x_a & y_a & z_a & 1 \\ x_b & y_b & z_b & 1 \\ x_c & y_c & z_c & 1 \\ x_d & y_d & z_d & 1 \end{pmatrix}\right|, \qquad V_{ivm} = S3\, V_{xyz}, \quad S3 = \sqrt{\frac{9}{8}} \tag{16}$$

Notes.

- Homogeneous determinant in Cartesian coordinates for tetra volume; conversion to IVM units uses $S3 = \sqrt{9/8}$ as used throughout.

See code: `tetra_volume_cayley_menger`. For tetrahedron volume background, see Tetrahedron – volume. Exact integer determinants in code use the Bareiss algorithm. External validation: these formulas align with implementations in the 4dsolutions ecosystem. See the Resources section for comprehensive details.

9.2 Fisher Information Matrix (FIM)

Background: Fisher information.

$$F_{i,j} = \mathbb{E}\left[\frac{\partial \log p(x;\theta)}{\partial \theta_i}\,\frac{\partial \log p(x;\theta)}{\partial \theta_j}\right] \tag{17}$$

Notes.

- Defines the Fisher information matrix as the expected outer product of score functions; see Fisher information.

Figure: empirical estimate shown in the FIM heatmap figure. See code: `fisher_information_matrix`.

See `src/information.py` — empirical outer-product estimator (`fisher_information_matrix`).

9.3 Natural Gradient

Background: Natural gradient (Amari).

$$\theta \leftarrow \theta - \eta\, F(\theta)^{-1}\, \nabla_\theta L(\theta) \tag{18}$$

Explanation.

- Natural gradient update: right-precondition the gradient by the inverse of the Fisher metric (Amari); see Natural gradient.

See code: `natural_gradient_step`.

See `src/information.py` — damped inverse-Fisher step (`natural_gradient_step`).

9.4 Free Energy (Active Inference)

$$\mathcal{F} = -\log P(o \mid s) + \mathrm{KL}[Q(s) \,\|\, P(s)] \tag{19}$$

Explanation.

- **Partition**: variational free energy decomposes into expected negative log-likelihood and KL between approximate posterior and prior; see Free energy principle.

See code: `free_energy`.

See `src/information.py` — discrete-state variational free energy (`free_energy`).

9.4.1 Figures

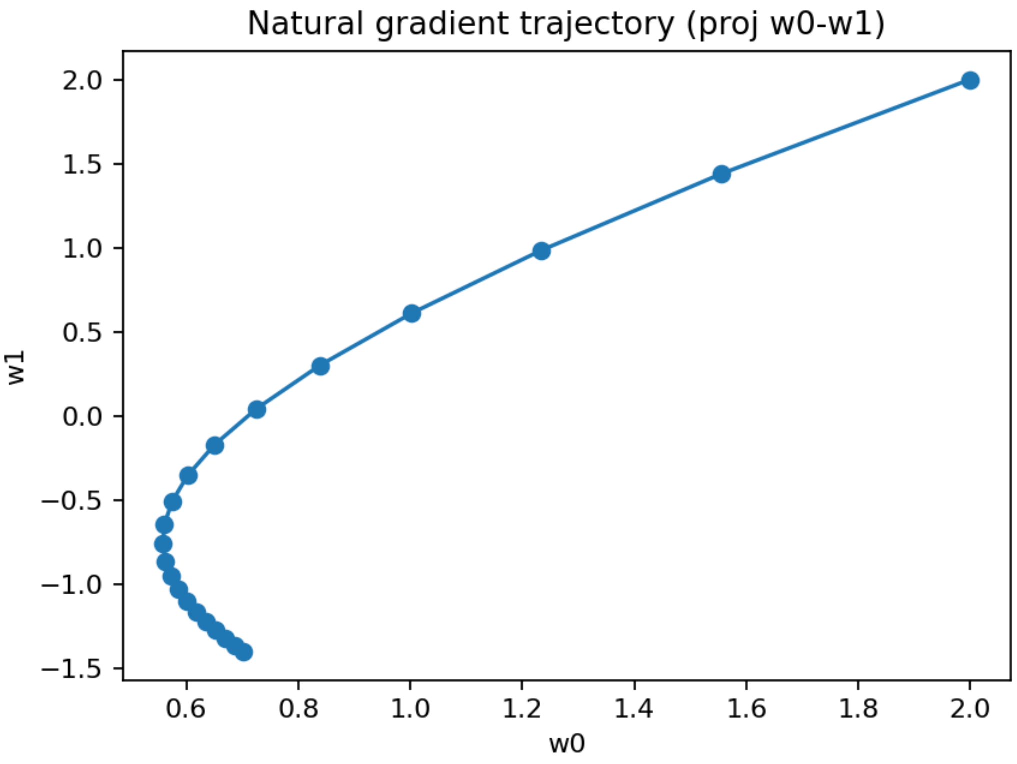

Figure 12: **Natural gradient trajectory demonstrating information-geometric optimization**. This trajectory shows natural gradient descent (Eq. 18) converging on a quadratic objective function. **Trajectory**: The blue line with markers traces the parameter evolution from initial guess to final optimum, showing the path taken through the 2D parameter space. **Markers**: Each marker represents one optimization step, with spacing indicating the step size and convergence rate. **Convergence behavior**: The trajectory shows smooth, direct convergence to the optimum, characteristic of natural gradient descent on well-conditioned objectives. **Comparison with standard gradient descent**: Natural gradient descent typically produces more direct trajectories than standard gradient descent, especially on ill-conditioned problems where the parameter space has strong anisotropy. This efficiency comes from the FIM-based scaling that adapts step sizes to local curvature. The trajectory demonstrates how information-geometric optimization leverages the intrinsic geometry of the parameter space to achieve faster, more stable convergence than naive gradient methods.

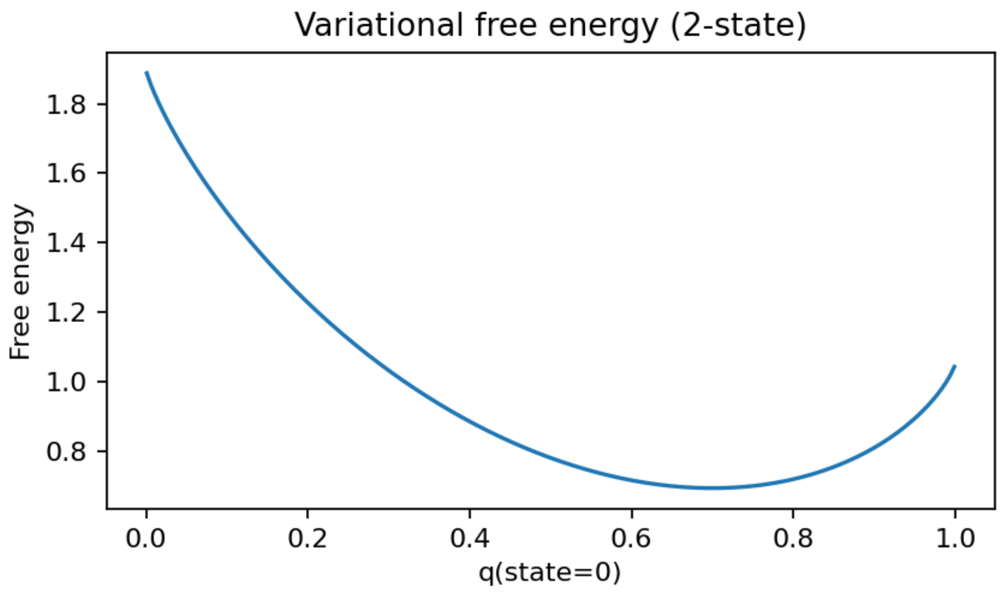

Figure 13: **Variational free energy functional for discrete binary states (Eq. 19)**. This curve illustrates the free energy landscape $\mathcal{F} = -\log P(o|s) + \mathrm{KL}[Q(s)||P(s)]$ as a function of the variational distribution parameter. **X-axis**: Variational parameter controlling the distribution over the two discrete states. **Y-axis**: Free energy value in natural units. **Curve shape**: The free energy exhibits a clear minimum at the optimal variational distribution, representing the best approximation to the true posterior given the constraints of the variational family. **KL divergence component**: The free energy balances data fit (first term) with regularization (KL divergence from prior), preventing overfitting while maintaining good predictive performance. **Optimization interpretation**: Minimizing this free energy corresponds to finding the best variational approximation to the true posterior, a fundamental task in Bayesian inference and active inference. The smooth, convex shape of the free energy landscape makes optimization straightforward using standard methods like gradient descent or natural gradient descent. This variational framework provides a principled approach to approximate inference in complex models where exact posterior computation is intractable.

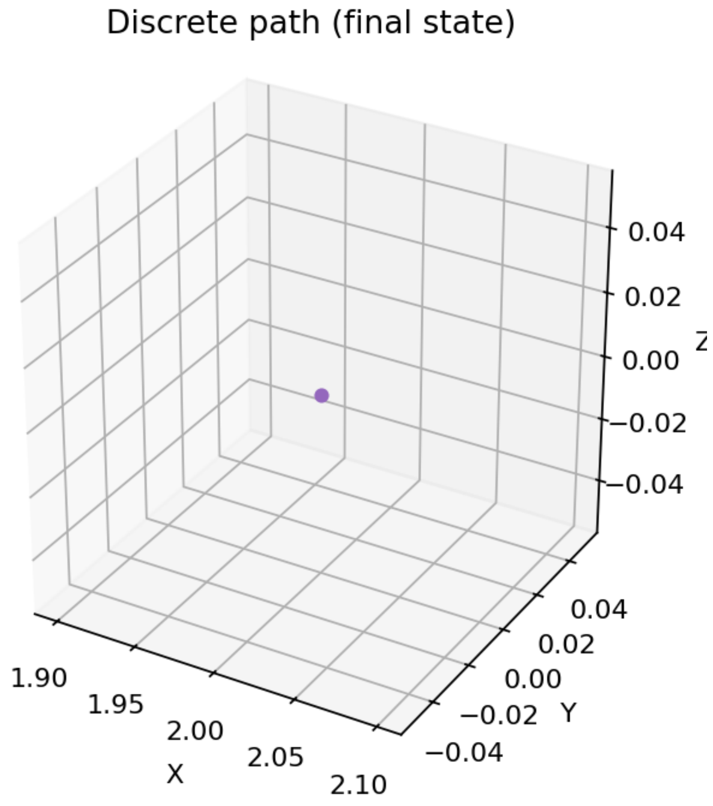

Figure 14: **Discrete IVM descent optimization path (final converged state)**. This static frame shows the final position of a discrete variational descent algorithm operating on the integer Quadray lattice. **Points**: Colored spheres representing the final optimization state, each positioned at integer Quadray coordinates projected to 3D space via the default embedding matrix. **Colors**: Each point has a distinct color for easy identification of different optimization components. **Optimization context**: These points represent the final state of the discrete IVM descent algorithm after converging to a local optimum on the integer lattice. The tight clustering of points indicates successful convergence, with the algorithm having found a stable configuration. **Lattice constraints**: All point positions correspond to integer Quadray coordinates, demonstrating the discrete nature of the optimization. The final configuration represents a stable "energy level" where further discrete moves do not improve the objective function. This visualization complements the time-series trajectory data and demonstrates the effectiveness of discrete optimization on the integer Quadray lattice.

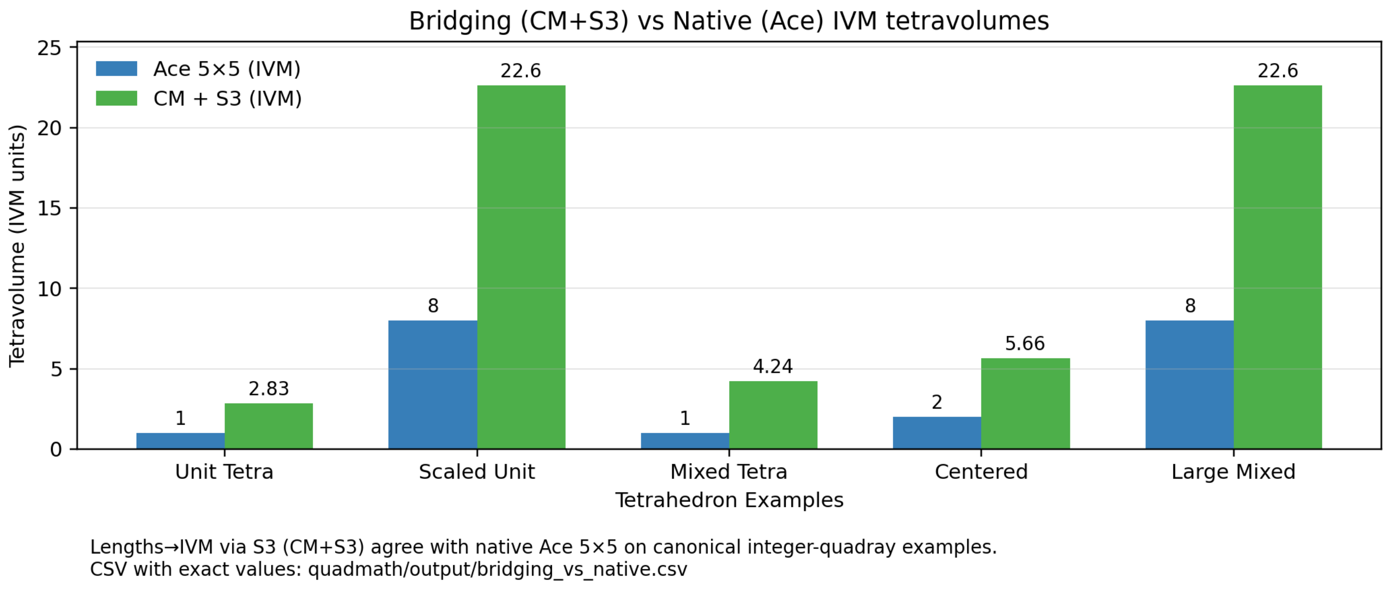

Figure 15: **Bridging (CM+S3) vs Native (Ace) IVM tetravolumes across canonical integer-quadray examples**. Bars compare V_{ivm} computed via Cayley–Menger on XYZ edge lengths with $S3 = \sqrt{9/8}$ conversion versus Tom Ace's 5×5 determinant formula operating directly on Quadray coordinates. **Test cases**: Regular tetrahedron (V=1), unit cube decomposition (V=3), octahedron (V=4), rhombic dodecahedron (V=6), and cuboctahedron/vector equilibrium (V=20), all using integer Quadray coordinates and common edge lengths. **Results**: The overlapping bars demonstrate numerical agreement at machine precision between the length-based Coxeter.4D approach (Cayley–Menger + S3 conversion) and the coordinate-based Fuller.4D approach (Ace 5×5), confirming the mathematical equivalence of these formulations under synergetics unit conventions. **Methodological significance**: This validation demonstrates that the bridging approach (converting from Euclidean to IVM units) produces identical results to the native IVM approach, supporting the use of both methods interchangeably depending on whether one has access to edge lengths or direct coordinates. Raw numerical data saved as `bridging_vs_native.csv` for reproducibility and further analysis.

9.5 Quadray Normalization (Fuller.4D)

Given $q = (a, b, c, d)$, choose $k = \min(a, b, c, d)$ and set $q' = q - (k, k, k, k)$ to enforce at least one zero with non-negative entries.

9.6 Distance (Embedding Sketch; Coxeter.4D slice)

Choose linear map M from quadray to $\mathbb{R}^3$ (or $\mathbb{R}^4$) consistent with tetrahedral axes; then $d(q_1, q_2) = \|M(q_1) - M(q_2)\|_2$.

9.7 Minkowski Line Element (Einstein.4D analogy)

$$ds^2 = -c^2\, dt^2 + dx^2 + dy^2 + dz^2 \tag{20}$$

Background: Minkowski space.

9.8 High-Precision Arithmetic Note

When evaluating determinants, FIMs, or geodesic distances for sensitive problems, use quad precision (binary128) via GCC's `libquadmath` (`__float128`, functions like `expq`, `sqrtq`, and `quadmath_snprintf`). See GCC libquadmath. Where possible, it is useful to use symbolic math libraries like SymPy to compute exact values.

9.8.1 Reproducibility artifacts and external validation

- **This manuscript's artifacts**: Raw data in `quadmath/output/` for reproducibility and downstream analysis:
  - `fisher_information_matrix.csv` / `.npz`: empirical Fisher matrix and inputs
  - `fisher_information_eigenvalues.csv` / `fisher_information_eigensystem.npz`: eigenspectrum and eigenvectors
  - `natural_gradient_path.png` with `natural_gradient_path.csv` / `.npz`: projected trajectory and raw coordinates
  - `bridging_vs_native.csv`: Ace 5×5 vs CM+S3 tetravolume comparisons
  - `ivm_neighbors_data.csv` / `ivm_neighbors_edges_data.npz`: neighbor coordinates (Quadray and XYZ)
  - `polyhedra_quadray_constructions.png`: synergetics volume relationships schematic
- **External validation resources**: The 4dsolutions ecosystem provides extensive cross-validation. See the Resources section for comprehensive details on computational implementations and validation.

9.9 Namespaces summary (notation)

- Coxeter.4D: Euclidean E^4; regular polytopes; not spacetime (cf. Coxeter, Regular Polytopes, Dover ed., p. 119). Connections to higher-dimensional lattices and packings as in Conway & Sloane.
- Einstein.4D: Minkowski spacetime; indefinite metric; used here only as a metric analogy when discussing geodesics and information geometry.
- Fuller.4D: Quadrays/IVM; tetrahedral lattice with integer tetravolume; unit regular tetrahedron has volume 1; synergetics scale relations (e.g., S3).

10 Appendix: The Free Energy Principle and Active Inference

10.1 Overview

The Free Energy Principle (FEP) posits that biological systems maintain their states by minimizing variational free energy, thereby reducing surprise via prediction and model updating. Active Inference extends this by casting action selection as inference under prior preferences. Background: see the concise overview on the Free energy principle and the monograph Active Inference (MIT Press).

This appendix emphasizes relationships among: (i) the four-fold partition of Active Inference, (ii) Quadrays (Fuller.4D) as a geometric scaffold for mapping this partition, and (iii) information-geometric flows (Einstein.4D analogy) that underpin perception–action updates. For the naming of 4D namespaces used throughout—Coxeter.4D (Euclidean E4), Einstein.4D (Minkowski spacetime analogy), Fuller.4D (Synergetics/Quadrays)—see `02_4d_namespaces.md`.

10.2 Mathematical Formulation and Equation Callouts (Equations linkage)

- Variational free energy (discrete states) — see Eq. (19) in the equations appendix, implemented by `free_energy`:

$$\mathcal{F} = -\log P(o \mid s) + \mathrm{KL}\big[Q(s) \,\|\, P(s)\big] \tag{21}$$

  where $Q(s)$ is a variational posterior, $P(s)$ a prior, and $P(o \mid s)$ the likelihood. Lower $\mathcal{F}$ is better.

- Fisher Information Matrix (FIM) as metric — see Eq. (17) in the equations appendix and `fisher_information_matrix` :

$$F_{i,j} = \mathbb{E}\left[\partial_{\theta_i} \log p(x;\theta)\; \partial_{\theta_j} \log p(x;\theta)\right]. \tag{22}$$

- Natural gradient descent under information geometry — see Eq. (18) in the equations appendix and `natural_gradient_step`; overview: Natural gradient:

$$\theta \leftarrow \theta - \eta\, F(\theta)^{-1}\, \nabla_\theta L(\theta). \tag{23}$$

Figures: See the Fisher Information Matrix and free energy figures in the optimization section above.

Discrete variational optimization on the quadray lattice: `discrete_ivm_descent` greedily descends a free-energy-like objective over IVM moves, yielding integer-valued trajectories. See the path animation artifact `discrete_path.mp4` in `quadmath/output/`.

10.3 Four-Fold Partition and Tetrahedral Mapping (Quadrays; Fuller.4D)

Active Inference partitions the agent–environment system into four coupled states:

- Internal (μ) — agent's internal states
- Sensory (s) — observations
- Active (a) — actions
- External (ψ) — latent environmental causes

See, for an overview of this partition and generative process formulations, the Active Inference review and the general entry on Active inference.

Tetrahedral mapping via Quadrays (Fuller.4D): assign each state to a vertex of a tetrahedron, using Quadray coordinates `(A,B,C,D)` with non-negative components and at least one zero after normalization. One canonical mapping is `A \leftrightarrow Internal (\mu)`, `B \leftrightarrow Sensory (s)`, `C \leftrightarrow Active (a)`, `D \leftrightarrow External (\psi)`. The edges capture the pairwise couplings (e.g., `\mu\text{--}s` for perceptual inference; `a\text{--}\psi` for control). Integer tetravolume then quantifies the "coupled capacity" region spanned by jointly feasible states in a time slice; see `Quadray` and tetravolume methods in `03_quadray_methods.md`.

Interpretation note: this Quadray-based mapping is a didactic geometric scaffold. It is not standard in the Active Inference literature, which typically develops the four-state partition in probabilistic graphical terms. Our use highlights structural symmetries and discrete volumetric quantities available in Fuller.4D, building on the computational foundations developed in the 4dsolutions ecosystem for tetrahedral modeling and volume calculations. See the Resources section for comprehensive details on the computational implementations.

Code linkage (no snippet): see `example_partition_tetra_volume` in `src/examples.py` and the partition tetrahedron figure above.

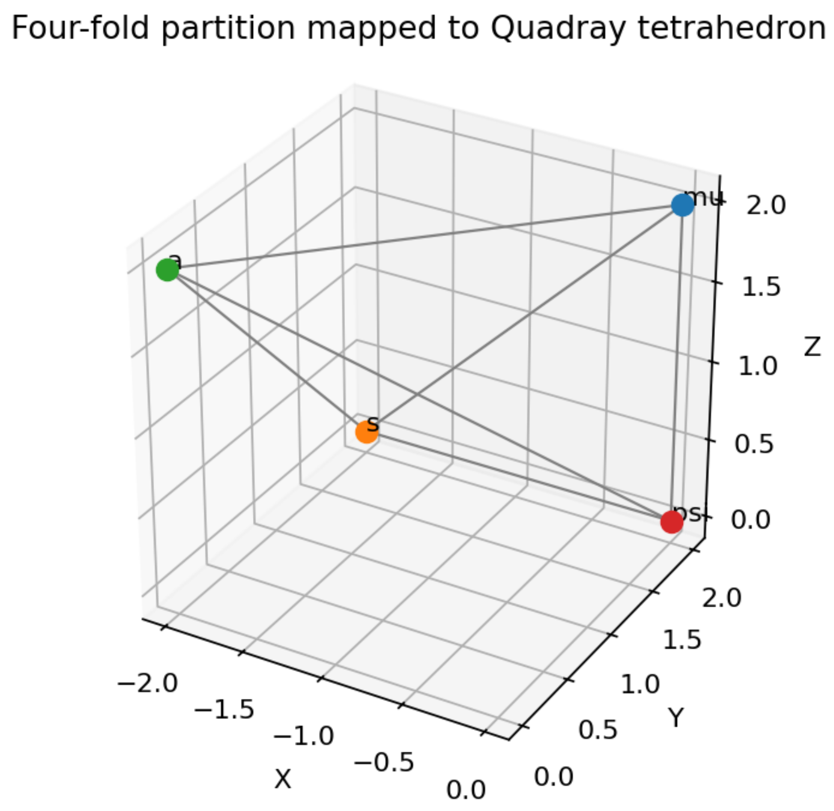

Figure 16: **Active Inference four-fold partition mapped to a Quadray tetrahedron in Fuller.4D**. This 3D tetrahedral visualization demonstrates the geometric embedding of Active Inference's fundamental four-fold partition within the Quadray coordinate system. **Tetrahedral structure**: The four vertices of the regular tetrahedron represent the four components of the Active Inference framework: perception, action, internal states, and external states. **Partition mapping**: Each face of the tetrahedron corresponds to a specific partition of the four-fold system, with the edges representing the relationships and interactions between different components. **Fuller.4D significance**: This geometric representation leverages the tetrahedral nature of Quadray coordinates to provide an intuitive visualization of the Active Inference framework's structure. The tetrahedron serves as a natural container for the four-fold partition, emphasizing the interconnected nature of perception, action, and state representation in active inference. **Optimization context**: The tetrahedral geometry also suggests natural optimization strategies that respect the four-fold structure, potentially leading to more efficient inference algorithms that leverage the geometric relationships between different components. This visualization demonstrates how the Fuller.4D framework can provide insights into complex systems like Active Inference through geometric intuition.

10.4 How the 4D namespaces relate here

- Fuller.4D (Quadrays): geometric embedding of the four-state partition on a tetrahedron; integer tetravolumes and IVM moves provide discrete combinatorial structure.
- Coxeter.4D (Euclidean E4): exact Euclidean measurements (e.g., Cayley–Menger determinants) for tetrahedra underlying volumetric comparisons and scale relations.
- Einstein.4D (Minkowski analogy): information-geometric flows (natural gradient, metric-aware updates) supply a continuum picture for perception–action dynamics.

The three roles are complementary: Fuller.4D encodes partition structure, Coxeter.4D provides exact metric geometry for static comparisons, and Einstein.4D guides dynamical descent.

10.5 Joint Optimization in the Tetrahedral Framework (Methods linkage)

- Perception: update μ to minimize prediction error on s under the generative model (descending $\nabla_{\mu} F$).
- Action: select a that steers ψ toward preferred outcomes (descending $\nabla_{a} F$).

Continuous-time flows (Einstein.4D analogy for metric/geodesic intuition): see `perception_update` and `action_update` in `src/information.py`. Discrete Quadray moves connect to these flows via greedy descent on a local free-energy-like objective; see `discrete_ivm_descent` in `src/discrete_variational.py` and the path artifacts in `quadmath/output/`.

10.6 Neuroscience and Predictive Coding

Under Active Inference, cortical circuits minimize free energy through recurrent exchanges of descending predictions and ascending prediction errors, aligning with predictive coding accounts. See the neural dynamics framing in Active Inference neural dynamics (arXiv:2001.08028).

10.7 Relation to Reinforcement Learning and Control

Active Inference replaces explicit value functions with prior preferences over outcomes and transitions, balancing exploration (epistemic value) and exploitation (pragmatic value) via expected free energy. See Active Inference and RL (arXiv:2002.12636). Connections to optimal control arise when minimizing expected free energy plays the role of a control objective; cf. Optimal control.

10.8 Links to Other Theories

- Bayesian Brain hypothesis: Bayesian brain
- Predictive Coding: Predictive coding
- Information Geometry: Fisher information, Natural gradient

10.9 Implications for AI and Robust Computation

FEP/Active Inference provide algorithms that unify perception and action under uncertainty, offering biologically plausible alternatives to standard RL with adaptive exploration and robust decision-making. See applications in AI (arXiv:1907.03876).

10.10 Code, Reproducibility, and Cross-References

– Equation references: Eq. (Free Energy), Eq. (FIM), Eq. (Natural Gradient) in `08_equations_appendix.md`. – Code anchors (for readers who want to run experiments): `free_energy`, `fisher_information_matrix`, `natural_gradient_step`, `perception_update`, `action_update`, and `discrete_ivm_descent` in `src/information.py` and `src/discrete_variational.py`.

Demo and figures generated by `quadmath/scripts/information_demo.py` output to `quadmath/output/`:

- **Visualizations**: `fisher_information_matrix.png`, `fisher_information_eigenspectrum.png`, `natural_gradient_path.png`, `free_energy_curve.png`, `partition_tetrahedron.png`.

- **Raw data**: `fisher_information_matrix.csv`, `fisher_information_matrix.npz` (F, grads, X, y, w_true, w_est), `fisher_information_eigenvalues.csv`, `fisher_information_eigensystem.npz`.
- **External validation**: Cross-reference with volume calculations and tetrahedral modeling tools from the 4dsolutions ecosystem. See the Resources section for comprehensive details.

11 Appendix: Symbols and Glossary

This appendix consolidates the symbols, variables, and constants used throughout the manuscript.

11.1 Sets and Spaces

Symbol	Name
$\mathbb{R}^n$	Euclidean space
IVM	Isotropic Vector Matrix
Coxeter.4D	Euclidean 4D (E^4)
Einstein.4D	Minkowski spacetime (3+1)
Fuller.4D	Synergetics/Quadray tetrahedral space

Descriptions:

- $\mathbb{R}^n$: n-dimensional real vector space.
- IVM: Quadray integer lattice (CCP sphere centers).
- Coxeter.4D: Four-dimensional Euclidean geometry (not spacetime); see Coxeter, Regular Polytopes (Dover ed., p. 119); related lattice/packing background in Conway & Sloane.
- Einstein.4D: Relativistic spacetime with Minkowski metric.
- Fuller.4D: Quadrays with projective normalization and IVM unit conventions.

11.2 Quadray Coordinates and Geometry

Symbol	Name	Description
$q = (a, b, c, d)$	Quadray point	Non-negative coordinates with at least one zero after normalization
A, B, C, D	Quadray axes	Canonical tetrahedral axes mapped by the embedding
k	Normalization offset	$k = \min(a, b, c, d)$ used to set $q' = q - (k, k, k, k)$
q'	Normalized Quadray	Canonical representative with at least one zero and non-negative entries
$P_0, \ldots, P_3$	Tetrahedron vertices	Vertices used in volume formulas
d_{ij}	Pairwise distances	Distance between vertices P_i and P_j (squared in CM matrix)
$\det(\cdot)$	Determinant	Determinant of a matrix
$\lvert\cdot\rvert$	Magnitude	Absolute value (determinant magnitude)
V_{ivm}	Tetravolume (IVM)	Tetrahedron volume in synergetics/IVM units; unit regular tetra has $V_{ivm} = 1$
V_{xyz}	Tetravolume (XYZ)	Euclidean tetrahedron volume

Symbol	Name	Description
$S3$	Scale factor	$S3 = \sqrt{9/8}$ with $V_{ivm} = S3\, V_{xyz}$ (synergetics unit convention)
Coxeter.4D	Namespace	Euclidean E^4; regular polytopes
Einstein.4D	Namespace	Minkowski spacetime (metric analogy only here)
Fuller.4D	Namespace	Quadrays/IVM; integer tetravolume
Eq. (lattice_det)	Lattice determinant	Integer-lattice volume via 3x3 determinant
Eq. (ace5x5)	Tom Ace 5x5	Direct IVM tetravolume from Quadrays
Eq. (cayley_menger)	Cayley–Menger	Length-based formula: 288 V^2 = det(·)

11.3 Optimization and Algorithms

Symbol	Name
α	Reflection coefficient
γ	Expansion coefficient
ρ	Contraction coefficient
σ	Shrink coefficient
V_{ivm}	Integer volume monitor

Descriptions:

- $\alpha, \gamma, \rho, \sigma$: Nelder–Mead parameters (typical values 1, 2, 0.5, 0.5).
- V_{ivm}: Tracks simplex volume across iterations.

11.4 Information Theory and Geometry

Symbol	Name	Description
log	Natural logarithm	Logarithm base e
$\mathbb{E}[\cdot]$	Expectation	Mean with respect to a distribution
$F_{i,j}$	Fisher Information entry	Empirical/expected $\mathbb{E}[\partial_{\theta_i} \log p\, \partial_{\theta_j} \log p]$; Eq. (17) in the equations appendix
$\mathcal{F}$	Variational free energy	$-\log P(o \mid s) + \mathrm{KL}[Q(s) \parallel P(s)]$; Eq. (19) in the equations appendix
$\mathrm{KL}[Q \parallel P]$	Kullback–Leibler divergence	$\sum Q \log(Q/P)$; information distance
$\nabla_\theta L$	Gradient	Gradient of loss L with respect to parameters θ (column vector)
η	Step size	Learning-rate scalar used in updates
θ	Parameters	Model parameter vector; indices θ_i

Symbol	Name	Description
ds^2	Minkowski line element	$-c^2\,dt^2 + dx^2 + dy^2 + dz^2$; Eq. (20) in the equations appendix
c	Speed of light	Physical constant appearing in Minkowski metric

11.5 Embeddings and Distances

Symbol	Name	Description
M	Embedding matrix	Linear map from Quadray to $\mathbb{R}^3$ (Urner-style unless noted)
$\lVert\cdot\rVert_2$	Euclidean norm	$\sqrt{x_1^2 + \cdots + x_n^2}$
R, D	Edge scales	Cube edge R and Quadray edge D with $D = 2R$ (common convention)

11.6 Greek Letters (usage)

Symbol	Name	Description
$\alpha, \gamma, \rho, \sigma$	NM coefficients	Nelder–Mead parameters (reflection, expansion, contraction, shrink)
θ	Theta	Parameter vector in models and metrics
μ	Mu	Internal states (Active Inference)
ψ	Psi	External states (Active Inference)
η	Eta	Step size / learning rate

11.7 Notes (usage and cross-references)

- **Figures referenced**: In-text references use LaTeX's automatic figure numbering for consistent cross-referencing.
- **Equation references**: Use labels defined in the text (e.g., Eq. (14) in the equations appendix).
- **Namespaces**: We use Coxeter.4D, Einstein.4D, Fuller.4D consistently to designate Euclidean E^4, Minkowski spacetime, and Quadray/IVM synergetics, respectively. This avoids conflation of Euclidean 4D objects (e.g., tesseracts) with spacetime constructs and synergetic tetravolume conventions.
- **External validation**: Cross-reference implementations from the 4dsolutions ecosystem for algorithmic verification and performance comparison baselines. See the Resources section for comprehensive details.

11.8 Acronyms and abbreviations

Acronym	Meaning
CM	Cayley–Menger (determinant-based tetrahedron volume)
PdF	Piero della Francesca (Heron-like tetrahedron volume)

Acronym	Meaning
GdJ	Gerald de Jong (Quadray-native tetravolume expression)
K-FAC	Kronecker-Factored Approximate Curvature (optimizer using structured Fisher)
CCP	Cubic Close Packing (same centers as FCC)
FCC	Face-Centered Cubic (same centers as CCP)
E^4	Four-dimensional Euclidean space (Coxeter.4D)
NM	Nelder–Mead (simplex optimization algorithm)
4dsolutions	Kirby Urner’s GitHub organization with extensive Quadray implementations
BEAST	Synergetic modules (B, E, A, S, T) in Fuller’s hierarchical system
OCN	Oregon Curriculum Network (educational framework integrating Quadrays)
POV-Ray	Persistence of Vision Raytracer (used in quadcraft.py visualizations)

11.9 API Index (auto-generated; Methods linkage)

The table below enumerates public symbols from `src/` modules.

Module	Symbol	Kind	Signature	Summary
`cayley_menger`	`ivm_tetra_volume_cayley_menger`	function	`(d2)`	Compute IVM tetravolume from squared distances via Cayley–Menger.
`cayley_menger`	`tetra_volume_cayley_menger`	function	`(d2)`	Compute Euclidean tetrahedron volume from squared distances (Coxeter.4D).
`conversions`	`quadray_to_xyz`	function	`(q, M)`	Map a `Quadray` to Cartesian XYZ via a 3x4 embedding matrix (Fuller.4D -> Coxeter.4D slice).
`conversions`	`urner_embedding`	function	`(scale)`	Return a 3x4 Urner-style symmetric embedding matrix (Fuller.4D -> Coxeter.4D slice).
`discrete_variational`	`DiscretePath`	class	`| Optimization trajectory on the integer quadray lattice. | | ` discrete_variational ` | `OptionalMoves` | class |`	

Module	Symbol	Kind	Signature	Summary
`discrete_variational`	`apply_move`	function	`(q, delta)`	Apply a lattice move and normalize to the canonical representative.
`discrete_variational`	`discrete_ivm_descent`	function	`(objective, start, moves=, max_iter=, on_step=)`	Greedy discrete descent over the quadray integer lattice.
`discrete_variational`	`neighbor_moves_ivm`	function	`()`	Return the 12 canonical IVM neighbor moves as Quadray deltas.
`examples`	`example_cuboctahedron_neighbors`	function	`()`	Return twelve-around-one IVM neighbors (vector equilibrium shell).
`examples`	`example_cuboctahedron_vertices_xyz`	function	`()`	Return XYZ coordinates for the twelve-around-one neighbors.
`examples`	`example_ivm_neighbors`	function	`()`	Return the 12 nearest IVM neighbors as permutations of {2,1,1,0} (Fuller.4D).
`examples`	`example_optimize`	function	`()`	Run Nelder–Mead over integer quadrays for a simple convex objective (Fuller.4D).
`examples`	`example_partition_tetra_volume`	function	`(mu, s, a, psi)`	Construct a tetrahedron from the four-fold partition and return tetravolume (Fuller.4D).
`examples`	`example_volume`	function	`()`	Compute the unit IVM tetrahedron volume from simple quadray vertices (Fuller.4D).
`geometry`	`minkowski_interval`	function	`(dt, dx, dy, dz, c)`	Return the Minkowski interval squared ds^2 (Einstein.4D).

Module	Symbol	Kind	Signature	Summary
glossary_gen	ApiEntry	class	| | | `glossary_gen` | `build_api_index` | function | `( src_dir)` | | | ` glossary_gen` | ` generate_markdown_table ` | function | `( entries)` | | | ` glossary_gen` | ` inject_between_markers ` | function | `( markdown_text, begin , end, payload)` | | | `information` | ` action_update` | function | `(action, free_energy_fn, step_size, epsilon)` | Continuous-time action update: da/dt = - dF/da. | | ` information` | ` finite_difference_gradient ` | function | `( function, x, epsilon )` | Compute numerical gradient of a scalar function via central differences. | | ` information` | ` fisher_information_matrix ` | function | `( gradients)` | Estimate the Fisher information matrix via sample gradients . | | `information` | `free_energy` | function | `( log_p_o_given_s, q, p)` | Variational free energy for discrete latent states. | | ` information` | ` natural_gradient_step ` | function | `( gradient, fisher, step_size, ridge)` | Compute a natural gradient step using a damped inverse Fisher. | | ` information` | ` perception_update` | function | `(mu, derivative_operator, free_energy_fn,	

Module	Symbol	Kind	Signature	Summary
`nelder_mead_quadray`	`centroid_excluding`	function	`(vertices, exclude_idx)`	Integer centroid of three vertices, excluding the specified index.
`nelder_mead_quadray`	`compute_volume`	function	`(vertices)`	Integer IVM tetra-volume from the first four vertices.
`nelder_mead_quadray`	`nelder_mead_quadray`	function	`(f, initial_vertices, alpha, gamma, rho, sigma, max_iter, tol, on_step)`	Nelder–Mead on the integer quadray lattice.
`nelder_mead_quadray`	`order_simplex`	function	`(vertices, f)`	Sort vertices by objective value ascending and return paired lists.
`nelder_mead_quadray`	`project_to_lattice`	function	`(q)`	Project a quadray to the canonical lattice representative via normalize.
`paths`	`get_data_dir`	function	`()`	Return `quadmath/output/data` path and ensure it exists.
`paths`	`get_figure_dir`	function	`()`	Return `quadmath/output/figures` path and ensure it exists.
`paths`	`get_output_dir`	function	`()`	Return `quadmath/output` path at the repo root and ensure it exists.
`paths`	`get_repo_root`	function	`(start)`	Heuristically find repository root by walking up from `start`.
`quadray`	`DEFAULT_EMBEDDING`	constant	`| | | `quadray` | ` Quadray` | class |`	Quadray vector with non-negative components and at least one zero (Fuller.4D).
`quadray`	`ace_tetravolume_5x5`	function	`(p0, p1, p2, p3)`	Tom Ace 5x5 determinant in IVM units (Fuller.4D).
`quadray`	`dot`	function	`(q1, q2, embedding)`	Return Euclidean dot product <q1,q2> under the given embedding.

Module	Symbol	Kind	Signature	Summary
`quadray`	`integer_tetra_volume`	function	`(p0, p1, p2, p3)`	Compute integer tetra-volume using det[p1-p0, p2-p0, p3-p0] (Fuller.4D).
`quadray`	`magnitude`	function	`(q, embedding)`	Return Euclidean magnitude ||q|| under the given embedding (vector norm).
`quadray`	`to_xyz`	function	`(q, embedding)`	Map quadray to R^3 via a 3x4 embedding matrix (Fuller.4D -> Coxeter.4D slice).
`symbolic`	`cayley_menger_volume_symbolic`	function	`(d2)`	Return symbolic Euclidean tetrahedron volume from squared distances.
`symbolic`	`convert_xyz_volume_to_ivm_symbolic`	function	`(V_xyz)`	Convert a symbolic Euclidean volume to IVM tetravolume via S3.
`visualize`	`animate_discrete_path`	function	`(path, embedding, save)`	Animate a point moving along a discrete quadray path.
`visualize`	`animate_simplex`	function	`(vertices_list, embedding, save)`	Animate simplex evolution across iterations.
`visualize`	`plot_ivm_neighbors`	function	`(embedding, save)`	Scatter the 12 IVM neighbor points in 3D.
`visualize`	`plot_partition_tetrahedron`	function	`(mu, s, a, psi, embedding, save)`	Plot the four-fold partition as a labeled tetrahedron in 3D.
`visualize`	`plot_simplex_trace`	function	`(state, save)`	Plot per-iteration diagnostics for Nelder–Mead.